

IS-4723

EFFICIENT SOLAR CELLS BY
SPACE PROCESSING

by

F. A. Schmidt
G. J. Campisi
A. J. Bevolo
H. R. Shanks
D. E. Williams

Materials Science Program
Ames Laboratory, USDOE
Iowa State University
Ames, Iowa 50011

FINAL REPORT

Contract No. H-34328B
October 1, 1978 to December 14, 1979

National Aeronautics and Space Administration
George C. Marshall Space Flight Center
Marshall Space Flight Center, AL 35812

DISTRIBUTION OF THIS DOCUMENT IS UNLIMITED

PLA

DISCLAIMER

This report was prepared as an account of work sponsored by an agency of the United States Government. Neither the United States Government nor any agency thereof, nor any of their employees, makes any warranty, express or implied, or assumes any legal liability or responsibility for the accuracy, completeness, or usefulness of any information, apparatus, product, or process disclosed, or represents that its use would not infringe privately owned rights. Reference herein to any specific commercial product, process, or service by trade name, trademark, manufacturer, or otherwise does not necessarily constitute or imply its endorsement, recommendation, or favoring by the United States Government or any agency thereof. The views and opinions of authors expressed herein do not necessarily state or reflect those of the United States Government or any agency thereof.

DISCLAIMER

Portions of this document may be illegible in electronic image products. Images are produced from the best available original document.

CONTENTS

	<u>PAGE</u>
ABSTRACT	iv
LIST OF FIGURES	v
LIST OF TABLES	vii
ACKNOWLEDGEMENT	viii
INTRODUCTION	1
BACKGROUND: EPITAXIAL SILICON THIN FILM GROWTH	4
A. Growth of Silicon on Silicon	5
B. Growth of Silicon on Sapphire, Graphite and Metals	7
EXPERIMENTAL APPARATUS AND PROCEDURE	9
A. Materials	9
(a). Silicon Source	9
(b). Molybdenum	9
(c). Tungsten	9
(d). Tantalum	10
(e). Molybdenum Disilicide	10
B. Apparatus	11
(a). Space Simulation Chamber	11
(b). Carrousel Assembly	11
(c). Silicon Deposition System	14
(d). Metal Evaporation Unit	17
C. Experimental Procedure	17
(a). General Deposition Procedure	17
(b). Specimen Analysis	19
1. Optical and Electron Microscopy	19
2. X-ray and Electron Diffraction Analysis	20
3. Surface Analysis	20
4. Electrical Measurements	20

	<u>PAGE</u>
RESULTS AND DISCUSSION	21
A. Tungsten Substrates	21
(a). Silicon Deposition Below 650°C	24
(b). Silicon Deposition Above 650°C	24
B. Molybdenum Substrates	29
(a). Silicon Deposited Below 670°C	30
(b). Silicon Deposited Above 670°C	32
C. Tantalum Substrates	32
D. Silicides	38
(a). Silicon Deposition on MoSi_2 Grown on Molybdenum	40
(b). Silicon Deposition on Large Grain Polycrystalline	48
MoSi_2 .	
1. Effects of Oxygen Partial Pressure	49
2. Effects of Temperature.	52
E. Electrical Characterization	59
SUMMARY AND CONCLUSION	62
RECOMMENDATIONS	65
BIBLIOGRAPHY	67

ABSTRACT

Thin films of electron beam evaporated silicon were deposited on molybdenum, tantalum, tungsten and molybdenum disilicide under ultrahigh vacuum conditions. Mass spectra from a quadrapole residual gas analyzer were used to determine the partial pressure of 13 residual gases during each processing step. Surface contamination and interdiffusion were monitored by in-situ Auger electron spectrometry. The substrates were characterized by x-ray analysis and SEM in the topographical and electron diffraction mode.

It was found that on polycrystalline tungsten with a {100} orientation, silicon was grown with a grain size measuring 3000 \AA in cross section and with {110} orientation below 630°C . At 670°C , silicon grains had grown to one micron in cross section and these grains had {111} and {110} orientations. On polycrystalline molybdenum substrates with {100} orientation, silicon grains measuring 2000 \AA across grew with a {110} orientation as high as 670°C . The presence of phosphorous in the silicon was responsible for attaining these elevated temperatures with silicide formations.

Heteroepitaxial silicon was grown on polycrystalline MoSi_2 at 800°C . The silicon grew on (111) MoSi_2 grains. This growth was sensitive to the presence of oxygen during deposition, the rate and length of deposition as well as the substrate orientation. Above 950°C silicon growth was no longer heteroepitaxial but crystals $80 \mu\text{m}$ in cross section were obtained. The presence of oxygen at a partial pressure of 1×10^{-10} Torr was found to reduce the size of silicon grains at 1100°C .

FIGURES

	<u>PAGE</u>
Figure 1. Carrousel and substrate holder assemblies used in the deposition and characterization of thin films of silicon on metal substrates.	12
Figure 2. A schematic of the heating oven assembly used to maintain substrate temperature.	13
Figure 3. A schematic of the silicon mold assembly for silicon vapor deposition.	16
Figure 4. A schematic of the metal evaporator unit for depositing contact electrodes on silicon.	18
Figure 5. SEM and optical photomicrograph of 1-01-1 showing a surface and edge view of fine grain {110} silicon on {100} tungsten.	25
Figure 6. SEM photomicrograph of the surface topography of silicon vacuum evaporated on tungsten substrate where the deposition temperature, T_D , was between 560°C and 850°C.	26
Figure 7. SEM photomicrographs of the surface topography of silicon deposited on molybdenum substrate at deposition temperature, T_D , (a) 550°C, (b) 670°C, (c) 750°C and (d) 850°C.	31
Figure 8. SEM photomicrograph of the surface and optical photomicrograph of the cross sectional profile of silicon deposited on tantalum in experiment 1-41-2.	35
Figure 9. SEM photomicrograph of the surface topography of silicon deposited on tantalum as a function of deposition temperature, T_D .	37
Figure 10. Optical photomicrograph of the cross sectional profile of samples 1-11-1, 1-11-2 and 1-11-3.	43
Figure 11. Optical photomicrograph of a cross sectional profile of silicon near the end of sample 1-11-3.	45
Figure 12. SEM photomicrographs of the surface of sample 1-91-3 showing silicon deposited on large grain molybdenum at elevated temperature.	46

	<u>PAGE</u>
Figure 13. Optical photomicrograph taken at 500X of silicon deposited on 1-61-3, 1-61-2, and 1-61-1 at substrate temperature, $T_D = 1100^\circ\text{C}$.	51
Figure 14. Optical photomicrograph of silicon deposited on MoSi_2 substrates at base pressure showing effects of temperature on grain growth.	53
Figure 15. A photograph of sample 1-71-2, taken at 6X, of silicon deposited at 800°C on MoSi_2 .	54
Figure 16. Optical photomicrograph of silicon deposited on MoSi_2 at 800°C on sample 1-71-2.	55
Figure 17. Optical photomicrograph of silicon deposited on MoSi_2 in experiment 1-111 at 800°C .	57
Figure 18. An optical photomicrograph of 1-111-2, taken at 50X, showing in the right corner heteroepitaxial $\{111\}$ silicon on MoSi_2 .	58
Figure 19. A plot of current density, J_F , versus forward bias voltage.	61

TABLES

<u>NUMBER</u>		<u>PAGE</u>
I.	Deposition Rates of Silicon Using Water-Cooled Mold Assembly.	15
II.	Experimental Condition for Annealing and Deposition of Silicon on Tungsten Substrates.	23
III.	Summary of the Results for X-Ray Analysis and Grain Size Measurements for Tungsten Substrates.	27
IV.	Experimental Conditions and Results for Silicon Deposited on Molybdenum.	33
V.	Experimental Conditions and Results for Silicon Deposited on Tantalum.	39
VI.	Experimental Conditions and Results for Experiment 1-11.	42
VII.	Experimental Conditions and Results of Silicon Deposited on Molybdenum in Experiment 1-91.	47
VIII.	Experimental Conditions and Results for Silicon Deposited on MoSi_2 .	50

ACKNOWLEDGEMENT

The authors and administrators of the Ames Laboratory, and in particular those of the Materials Science Program, wish to gratefully acknowledge Dr. J. R. Carruthers of the National Aeronautics and Space Administration for his interest in and support of this work. We appreciate the efforts of Dr. W. A. Oran, Dr. R. J. Naumann, Mr. J. R. Williams and Mr. W. Moore of the George C. Marshall Space Flight Center for their suggestions and excellent cooperation during the period of this work.

We also wish to acknowledge Dr. J. D. Verhoeven, Mr. E. D. Gibson, Mr. O. D. McMasters, Mr. D. K. Rehbein, Mr. M. E. Thompson and Mr. H. H. Baker of the Ames Laboratory for their consultations and assistance throughout this study.

This work was performed in the Ames Laboratory, operated by the U.S. Department of Energy, Contract No. W-7405-ENG-82.

INTRODUCTION

The purpose of this work is to design and define a laboratory experiment that demonstrates the feasibility of preparing efficient Schottky barrier solar cells (SBSC) by space processing. The investigation is directed toward utilizing the non-contaminating space environment in the preparation of thin film silicon solar cells by epitaxial growth on various metal substrates. The resulting deposits are then characterized to determine which parameters are essential to enhance solar cell efficiency.

Polycrystalline solar cells have the potential to reduce the cost of photovoltaic generated electricity,¹ but they presently suffer from low output efficiency and a lack of a viable method of mass production. In the SBSC, a metal-semiconductor contact provides the built-in voltage required to separate the photogenerated electron-hole pairs. Several researchers^{2,3} have reported high efficiencies (> 10%) for the SBSC on single-crystal silicon. More recently Chu⁴ has reported 9% efficiency of p-n junction type polycrystalline silicon solar cells. The SBSC device, however, utilizes the metal semiconductor contact and avoids the diffusion or implantation doping necessary to form the bipolar p-n junction device.

The most economic fabrication scheme for SBSC will probably involve the deposition of silicon, in polycrystalline form, onto a suitably prepared metal substrate. The physical properties of the metal-semiconductor system that enhance the device efficiency are (1) the silicon-metal contact must produce a high Schottky barrier near 1.0 eV and (2) the substrate must permit the growth of large grains of polycrystalline silicon measuring $\sim 100 \mu\text{m}$ in cross section and $\sim 10 \mu\text{m}$ thick.

The ambient gases present during the deposition of silicon onto metal substrates can greatly influence the nature of the deposit obtained. These gases can serve as contaminants which drastically alter the electrical properties of the metal-silicon interface through their influence on the surface states. Even submonolayer quantities can alter the Schottky barrier height by several hundred millivolts and seriously reduce the efficiency of the device. In addition, the presence of adsorbed contamination on the metal surface can profoundly influence the critical nucleation stages of the growth of the silicon film resulting in a reduction in grain size that can lower the efficiency of the device. Further, these contaminants can become incorporated into the growing silicon film and thereby influence its grain structure or electrical properties.

Previous research in our Laboratory⁵ indicates that the formation of metal silicides has been a serious impediment to the growth of polycrystalline silicon films on cleaned metal substrates. At temperatures low enough to retard silicide growth the silicon films are very fine grained (<1 μm). As a result, the electrical properties of the films are dominated by grain boundary phenomenon, and the determination of the Schottky barrier height has been impossible. If the temperature is increased to encourage grain growth, the formation of metal silicide becomes so rapid that no free silicon remains on the surface.

During the period of this report silicon has been deposited on substrates of tungsten, molybdenum, tantalum and MoSi_2 . A simulated non-contaminating space environment was used to systematically study the effect of various gases on the efficiency of SBSC formed by the evaporation of silicon on these substrates. The polycrystalline grain size of the silicon

layer was determined as a function of oxygen partial pressure and conditions for heteroepitaxial growth on metallic substrates was studied. Profound influences were discovered on the silicon grain size due to oxygen partial pressure, substrate temperature, and substrate orientation. Controlling these variables has resulted in silicon films that are single crystalline with a cross-section of several millimeters which is more than adequate for solar cell fabrication.

BACKGROUND: EPITAXIAL SILICON THIN FILM GROWTH

This section is intended to review⁶ the progress of the last 25 years in thin film silicon growth on substrates such as silicon, ceramics and metals. In the first subsection, the growth of silicon on silicon is reviewed since this system is the most extensively studied and the growth mechanisms for it are applicable to other substrates. The second subsection describes silicon growth on sapphire, ceramics, graphite and a review of silicon growth on metals.

The two principal methods in use today to obtain thin films of silicon are (1) chemical vapor deposition and (2) vacuum evaporation. Commercially, the chemical vapor deposition technique has been preferred since it does not require ultrahigh vacuum equipment and rapid growth rates of one micron/min are routinely obtained. For the silicon growth studies, the vacuum evaporation technique has been a more desirable method since it has provided a controlled environment in which the deposit could be monitored with surface sensitive instruments. The availability of ultrahigh vacuum (UHV) systems and surface analysis techniques such as low energy electron diffraction (LEED) and Auger Electron Spectroscopy (AES) have provided in-situ analyses during the various stages of growth which consequently have lead to advances in the understanding of the growth process.

Before proceeding further, it is necessary to clarify the term "epitaxy". In general, epitaxy means an oriented or single crystal growth of one material upon another such that a crystallographic relationship between the grown layer and the substrate exists. When the oriented single crystal is grown on an oriented substrate of the same material, this is

referred to as homoepitaxy, such as silicon on silicon. If the oriented single crystal is grown on a substrate of different material, it is called heteroepitaxy.

A. Growth of Silicon on Silicon.

The mechanism whereby homoepitaxial growth of silicon could proceed has been described by Burton, Cabrera and Frank.⁷ This growth was described as proceeding by monoatomic steps if the surface was "atomically" or "ultra" clean and smooth. During deposition, silicon atoms are adsorbed on the surface where they diffuse across the surface to a step or are reevaporated in a finite time. In order for the epitaxial growth to proceed, it is necessary to have a sufficient number of dislocations at the surface to provide a source of steps. A slight misalignment from the preferred (111) can relax the need for surface dislocations. The process of growth along steps is known as two dimensional growth since it describes a planar process. On the other hand, the three dimensional growth process occurs when silicon nucleates and grows in clusters that eventually coalesce into the continuous film. This type silicon growth on the (111) silicon substrate has been described by Unvala and Booker.⁸ In a subsequent paper,⁹ these authors reproduced the three dimensional cluster growth at substrate temperatures of 1100°C. They found however, that by increasing the deposition rate at this temperature, they produced films that were continuous, uniform and exhibiting a lower number of stacking faults than the low rate material. Widmer¹¹ found no three dimensional growth when he grew thin films of silicon at temperatures of only 700°C and deposition rates of 300 Å/min in an ultrahigh vacuum of 10^{-11} Torr.

To study the details of thin film growth and the surface conditions that control this growth, three surface sensitive techniques have been

generally employed with exceptional results. These techniques are (1) low energy electron diffraction (LEED), (2) reflection high energy electron diffraction (RHEED) which provide structural data about early stages of film growth and (3) Auger electron spectroscopy (AES) which can detect the chemical composition and residual contamination on the surface. The initial LEED studies were made by Jona^{11,12} in which he obtained silicon (111) - 7 x 1 patterns by vacuum evaporation on clean silicon with a (111) orientation by slowly depositing silicon at 0.6 $\text{\AA}/\text{min}$ with the substrate held at 400°C.

Surface contaminants such as oxygen and carbon have been shown to play a significant role in inhibiting two dimensional homoepitaxial growth. Oxygen is present on the surface as adsorbed oxygen or as SiO_2 . Conversely, the role of carbon in the promotion of three dimensional growth was extensively studied by several investigators¹³⁻¹⁶ who found that it was difficult to remove the residual carbon layer unless the heat treatment of the silicon was in excess of 1200°C. Although carbon could be removed by diffusion into the bulk or by reaction with the gases in the vacuum chamber, β -SiC precipitates were found at the surface after a 1200°C heat treatment. These precipitates gave rise to three dimensional growth. Henderson and Helm¹⁵ further stated that any form of adsorbed carbon on the surface would probably produce the same growth effect as β -SiC precipitates.

To study the effects of adsorbed carbon in the growth of silicon, Joyce et al.^{17,18} recontaminated an atomically clean silicon surface with ethylene and measured the changes in the three dimensional growth as a function of ethylene exposure. The lateral growth of the silicon grains was impeded by increased nucleation sites arising from the higher carbon surface contamination.

The second major contamination that affects the epitaxial growth of silicon is oxygen present either as SiO_2 or adsorbed on the surface. The deleterious effects of oxygen are especially evident during the deposition in which the substrate temperature and silicon arrival rate are low. The investigations^{19,20} into this effect concluded that at low deposition rates and temperatures below 900°C , silicon reacted with SiO_2 slowly to form volatile SiO , and the deposition could not proceed until all the SiO_2 was removed. The interval before deposition was referred to as the induction period, and the duration of this period was proportional to the deposition rate and exponentially dependent on temperature.

B. Growth of Silicon on Sapphire, Graphite and Metals.

Significant interest in ceramic substrates especially $\alpha\text{-Al}_2\text{O}_3$, sapphire, has been generated from the use of thin film silicon in the fabrication of MOS transistors, diodes, bipolar transistors and integrated circuits. On ceramic substrates, the thin silicon films are grown by chemical vapor deposition; however, the vacuum evaporation technique was preferred in growth studies. Milek²¹ and Filby and Nelson²² have compiled an extensive review of the literature of silicon on ceramics with special emphasis given to silicon on sapphire.

Using LEED and AES, Chang²³ has made a careful study of the conditions that produced epitaxial silicon by vacuum evaporation on $(\bar{1}012)$, $(11\bar{2}3)$, (0001) and $(11\bar{2}0)$ sapphire surfaces. To achieve heteroepitaxial growth, the substrate temperature was maintained below 925°C to prevent the silicon reaction with Al_2O_3 . The products of this reaction are volatile SiO , oxides of aluminum and residual aluminum that could lead to the autodoping of silicon. The highest quality films were grown in the (100) orientation on

the (1012) sapphire plane between 650°C and 925°C.

Silicon has also been grown on spinels, SiO_2 , BeO , SiC and glazed ceramics but the results have been only partially successful in obtaining high quality heteroepitaxial silicon films.

Graphite substrates have been used by Chu²⁴ for silicon growth by chemical vapor deposition in photovoltaic applications. The silicon deposit was polycrystalline with the microstructure dependent on deposition rate and substrate temperature. Silicon crystallites as large as 30-40 μm were grown but these films have proved unsuitable for high efficiency solar cells due to excess recombination at the grain boundaries.

In general epitaxial growth of silicon on metals has been avoided due to the problems of lattice mismatch, thermal expansion differences and metal-silicon alloying. Initial studies by Jona^{25,26,27} of silicon on aluminum, nickel and beryllium were intended as a LEED study of silicon on these metals and were not an attempt to attain epitaxial growth. Polycrystalline silicon has been grown on large grain polycrystalline tungsten by Bevolo et al.⁵ under UHV conditions. They found that the polycrystalline silicon could be grown at substrate temperatures below 625°C but the crystallite size was only 3000 \AA in cross section. Above 625°C, tungsten silicides were formed. In a similar experiment Racette and Frost²⁸ found that it was possible to grow {110} silicon on 35-60 μm {100} tungsten grains. Initially they claimed that the polycrystalline silicon was comparable to the substrate grain size but subsequent transmission electron microscopy indicated submicron crystallites which was in essential agreement with Bevolo et al.⁵

EXPERIMENTAL APPARATUS AND PROCEDURE

In the following subsections, the materials, apparatus and experimental procedure used to deposit silicon under low pressure conditions onto various metallic substrates are described.

A. Materials.

(a) Silicon Source. Two silicon ingots were used in these deposition experiments. The first ingot was obtained from the Dow Corning Corp. and was high purity p-type silicon with a resistivity of 13 to 15 ohm-cm. It was used in the experiments 1-01 through 1-31 and was designated Silicon I. An n-type silicon ingot was used for Experiment 1-41 and in all subsequent experiments. This ingot was phosphorus doped with 0.008 ohm-cm resistivity and was designated Silicon II. It was obtained from the Wacker Chemical Co., Munich, Germany.

(b) Molybdenum. The molybdenum substrates used in this investigation were prepared from 0.013 cm thick sheet obtained from the Molybdenum Corporation of America. It contained 8 ppma (parts per million atomic) nickel, 10 ppma potassium, 20 ppma aluminum, 31 ppma tungsten, 40 ppma iron, 50 ppma zirconium, 50 ppma silicon, 50 ppma carbon, 100 ppma nitrogen and 120 ppma oxygen. The molybdenum substrates measured 1.4 x 2.2 x 0.013 cm and were electropolished prior to a vacuum anneal at 1100°C. The recrystallized molybdenum grains measured between 10 and 60 μm in cross section and were predominantly oriented along the {100} plane.

(c) Tungsten. Tungsten substrates were prepared from 0.013 cm thick sheet that was obtained from the Rembar Company. The material contained 15

ppma carbon, 185 ppma oxygen, and 15 ppma nitrogen. The major metallic impurities included 10 ppma aluminum, 10 ppma chromium, 100 ppma iron, 170 ppma molybdenum, 70 ppma niobium, 60 ppma nickel, and 60 ppma titanium. The substrates measured 1.4 x 2.2 x 0.13 cm and were electropolished. As received, the tungsten was fine grained (< 5 μ m). However, with vacuum annealing, the recrystallized tungsten grains measured 5 to 60 μ m in cross section and were also oriented along the {100} plane.

(d) Tantalum. The tantalum substrates were sheared from 0.013 cm sheet that was obtained from the Kawecki Berylco Company. The major metallic impurities in the material were determined to be 5 ppma chlorine, 7 ppma chromium, 70 ppma iron, 10 ppma potassium, 9 ppma sodium, 31 ppma nickel and 110 ppma silicon. The carbon, oxygen and nitrogen content was 660 ppma, 1075 ppma, 130 ppma respectively. The substrates were electropolished in a sulfuric-methanol bath. The recrystallization of the substrates was performed in-situ at 1700°C for 360 min and the resulting grains were found to be oriented in the {211} and {111} planes.

(e) Molybdenum Disilicide (MoSi₂). Small ingots of molybdenum disilicide were produced in our Laboratory by arc melting stoichiometric amounts of molybdenum and high purity silicon. Substrates were cut from these ingots into wafers 1.1 to 1.5 cm in diameter and 0.05 to 0.10 cm thick. These wafers were mechanically polished flat on one face through Linde A and B. The MoSi₂ grains varied between 0.01 to 0.5 cm in cross section and showed no preferred orientation.

B. Apparatus.

The experimental system used for the deposition of silicon consists of the space simulation chamber (SSC), the analytic instruments, the silicon deposition assembly, the substrate holder assembly and the metallization unit.

(a) Space Simulation Chamber. The stainless chamber, equipped with cryosorption, titanium sublimation and differential ion pumps and a large liquid nitrogen cryopanel, routinely attains a pressure of 5×10^{-11} to 5×10^{-12} Torr (N_2) after a 380°C bakeout for 7 days. The residual gas pressures were measured with an ionization gauge and a UTI Model 100C residual gas analyzer. The details of the vacuum system and the residual gas pressure calculation were described in an earlier work.⁵ An Auger electron spectrometer (AES) was also mounted in the vacuum chamber to provide in-situ analysis of the specimen surface.

(b) Carrousel Assembly. The carrousel, shown in Figure 1, was attached to a specimen manipulator that was obtained from Physical Electronics Inc. The carrousel contains three substrates, thermocouples, and attached power cables. The substrates had a thermocouple spot welded to their back side. An oven assembly, shown in Figure 2, was built to allow for the indirect heating of substrates that were non-metallic, brittle or irregularly shaped. The substrate was sandwiched between two tantalum sheets, whose edges were crimped into slotted tantalum flats that were ordinarily used to fasten the substrates to the carrousel. The top sheet contained a 0.95 cm diameter hole and was wider so that a uniform cross sectional area was maintained. Silicon could then be deposited through the hole onto the substrate. A thermocouple was placed between the substrate and the bottom tantalum sheet

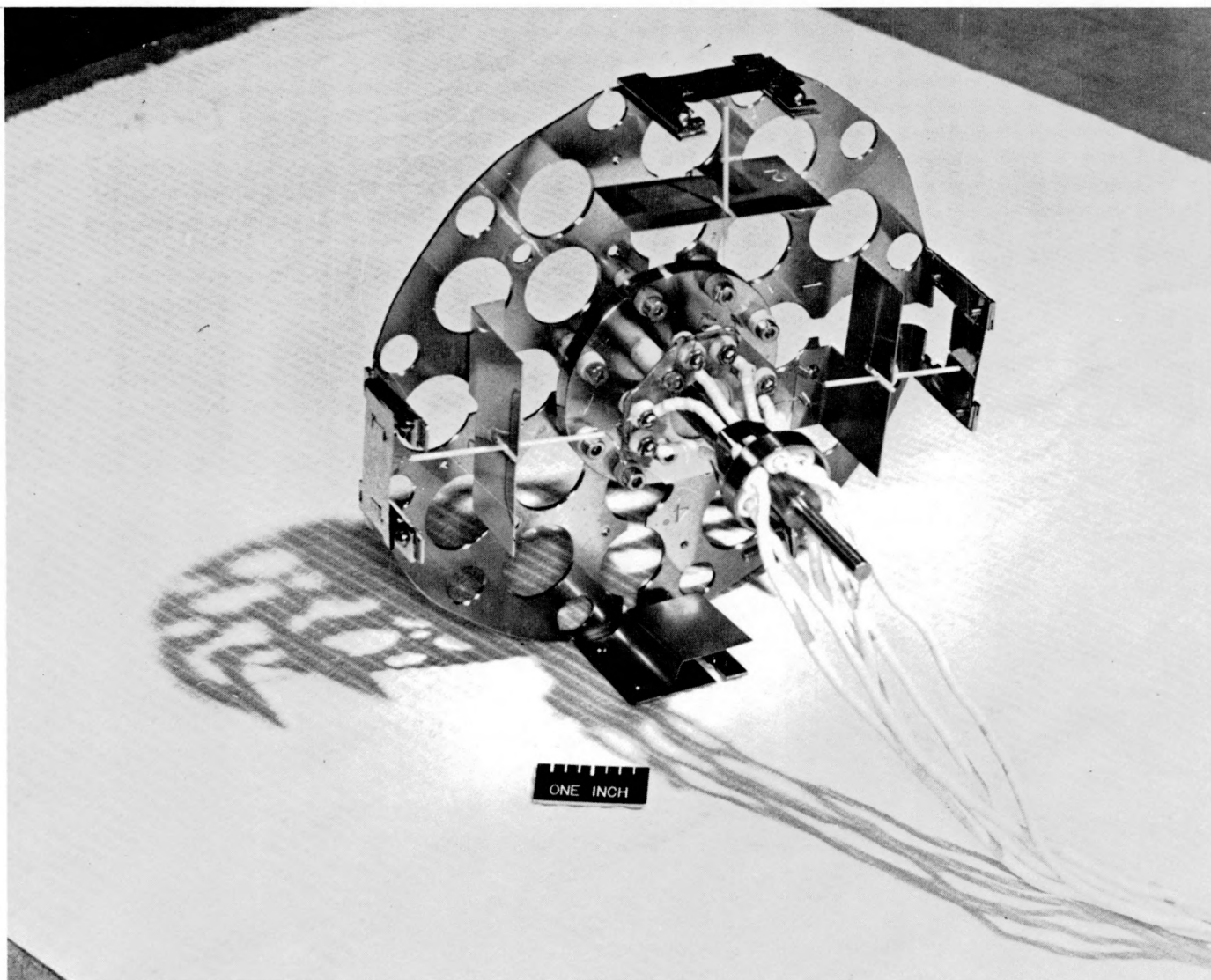


Figure 1. Carrousel and substrate holder assemblies used in the deposition and characterization of thin films of silicon on metal substrates.

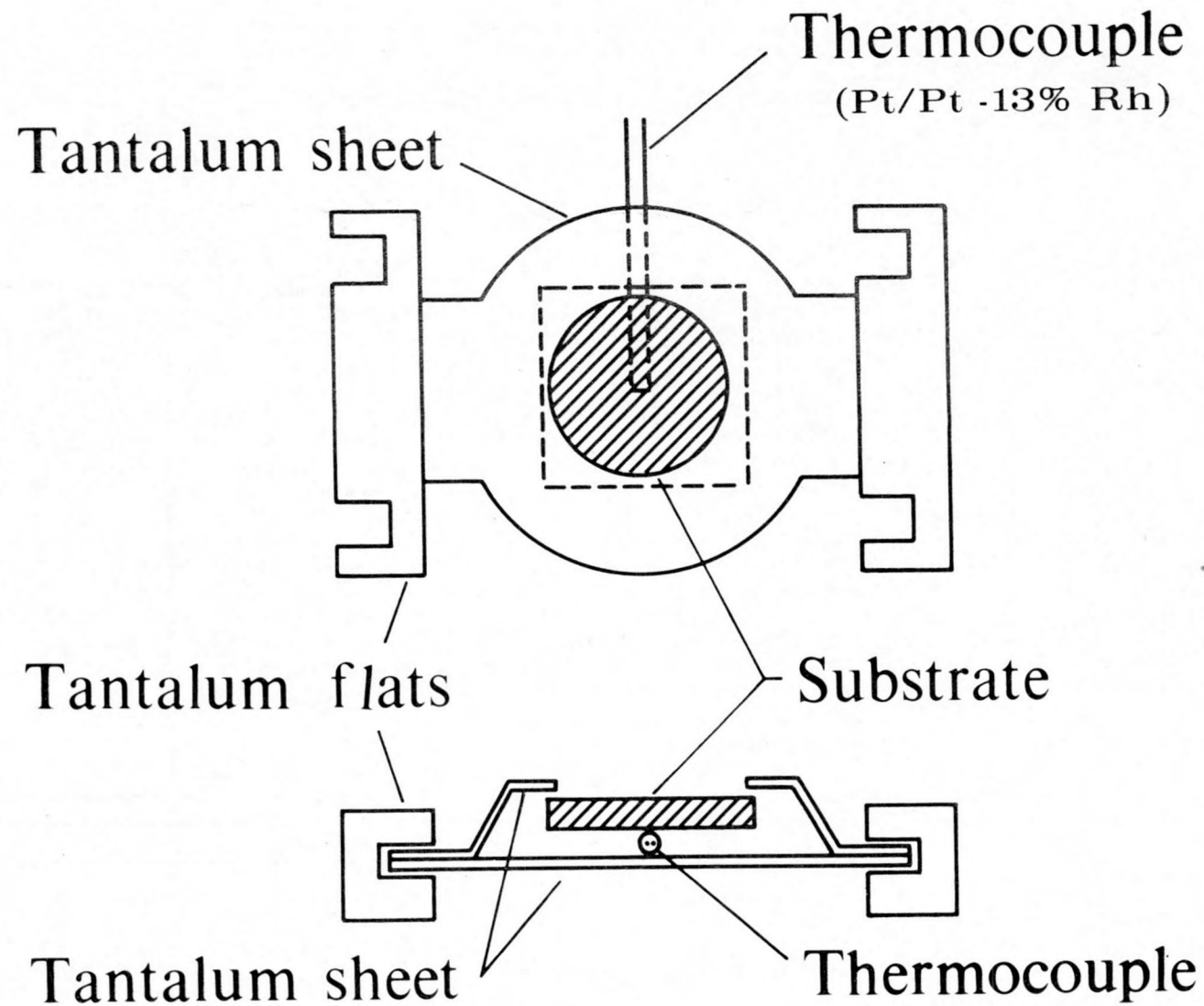


Figure 2. A schematic of the heating oven assembly used to maintain substrate temperature.

to monitor temperature changes of the substrate. For most applications, a Pt/Pt-13% Rh thermocouple was used.

The oven was tested successfully using a single crystal silicon wafer as a substrate. In this experiment, 1-41-2, silicon was deposited on the wafer for 300 minutes at 150 \AA/min with the wafer temperature maintained at 800°C . Electron channeling of the substrate and the silicon film layer indicated perfect registry of the epitaxial film on the substrate.

In several experiments, specifically those with the tungsten substrates, where it was necessary to recrystallize the substrate in-situ at temperatures greater than 1700°C , a combination of optical and infrared pyrometry and thermocouples were required to cover the full temperature range under the given conditions. A Raytek Thermoalert infrared pyrometer, Model 300, was calibrated against the Pt/Pt-13%Rh thermocouples between 400 and 800°C prior to the anneal of each substrate. At the annealing temperature the thermocouples became inoperative and the optical pyrometer was substituted. For the deposition, the infrared pyrometer calibrated for the specific substrate was then employed to set and monitor the desired temperature.

(c) Silicon Deposition System. Silicon was evaporated from the top of the ingot that was heated by an electrostatically focused, 6-KW Pierce type electron beam gun that was obtained from the Veeco Co. In this manner crucible contamination to the silicon was minimized. A water cooled hearth installed after experiment 1-11, supported the silicon and served several functions; (1) the deposition rate could be dramatically increased, (2) contamination of the silicon from the hearth was eliminated and (3) an overflow of molten silicon from the top of the ingot did not lead to catastrophic

alloying with the vacuum chamber walls. The design of the mold assembly is shown schematically in Figure 3. The silicon ingot which measured 3.2 cm in diameter and 5 to 7 cm high, rested on the tantalum hearth. This hearth was supported by a cylindrical stainless steel pedestal. The cylindrical pedestal was welded to a water feedthrough and mounted on a high vacuum flange. The entire pedestal unit could be inserted through a 3.7 cm tube in the bottom of the chamber.

The silicon deposition rates using the water-cooled mold assembly were determined by evaporating silicon on three electropolished molybdenum substrates with the SSC pressure maintained at 10^{-7} Torr. A tantalum band was attached across the center of each substrate to provide a well defined edge in the silicon film for the Dektak profile measurements. Silicon depositions were made on the three substrates for 30 minutes using 1000, 1250 and 1500 watts of electron beam power. As can be seen in Table I, deposition rates up to 7500 \AA/min were obtained with the new mold assembly.

Table I. Deposition rates of silicon using water-cooled mold assembly.

Electron Beam Power (watts)	Thickness (μm)	Time (min)	Rate (\AA/min)
1000	2.0	32	630
1250	7.9	30	2600
1500	22	30	7500

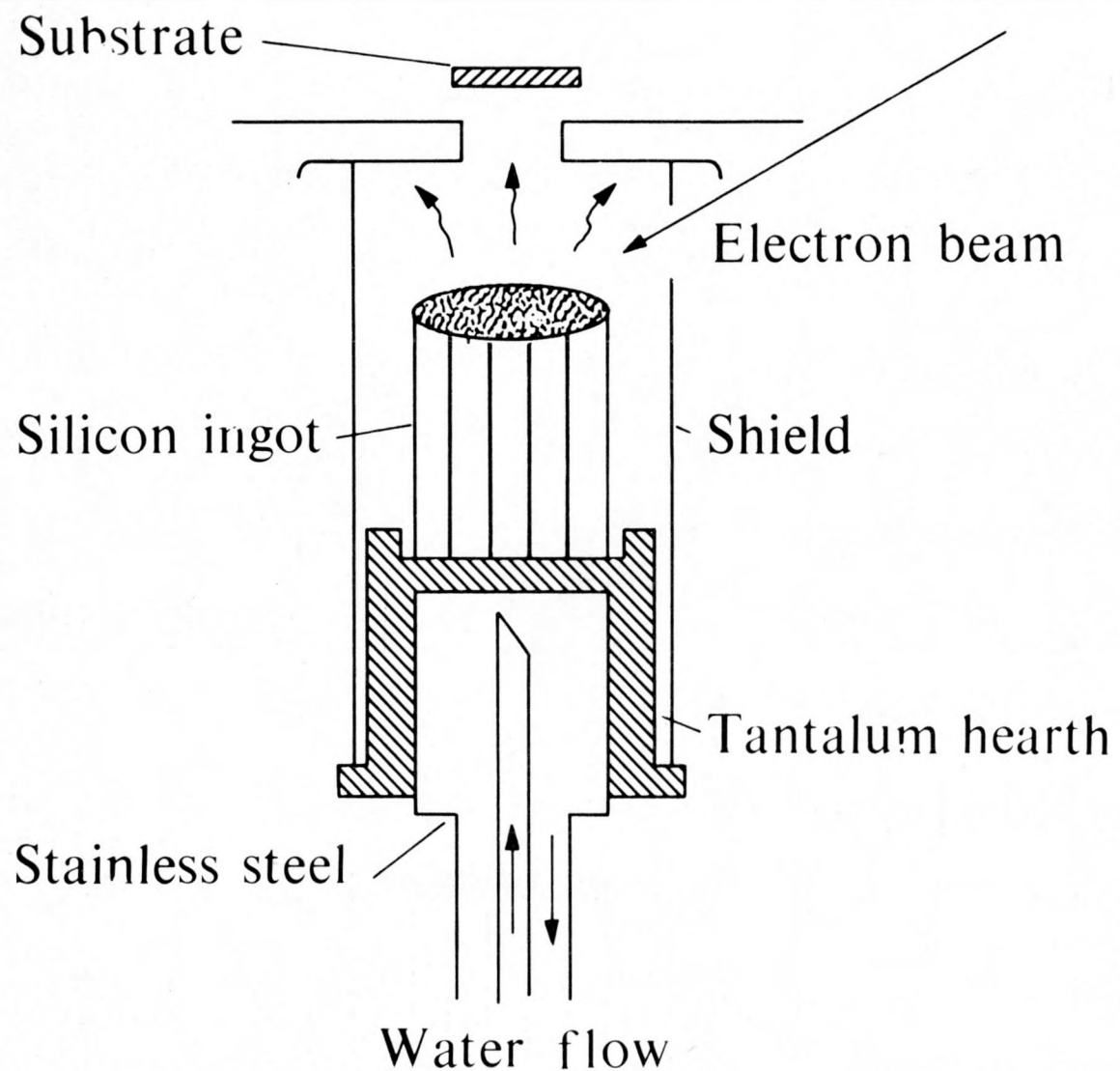


Figure 3. A schematic of the silicon mold assembly used for silicon vapor deposition.

(d) Metal Evaporator Unit. An evaporator unit was installed in the SSC to provide in-situ metal films on the clean electron beam deposited silicon. Electrical contacts were prepared by evaporating gold from a tungsten boat at an oblique angle through an appropriate mask onto the silicon deposit. The components of this unit are shown in Figure 4. The dual electrical feedthrough was mounted on the stainless steel frame and provided a convenient method for electrically isolating the source boat. The tungsten boat was connected to the copper electrodes of the feedthrough by means of tantalum tabs. The tungsten boat was crimped into slotted tantalum flats which were attached to the tantalum electrodes. The source boat measured 5 cm long by 1.3 cm wide by 0.013 cm thick. Braided copper cables provided the power leads between the electrical feedthroughs mounted on the chamber wall and the evaporator unit. A protective vapor shield surrounded the entire unit confining the deposit to the mask region. A mirror was set above the vapor shield so that the metal evaporation process could be observed.

C. Experimental Procedure.

(a) General Deposition Procedure. The substrate, onto which silicon was to be deposited, was attached to the carrousel, and the entire assembly loaded in the SSC. The chamber was then evacuated, baked out at 380°C for 7 days and cooled to room temperature. After bakeout, the pressure in the chamber was 1×10^{-10} Torr or lower and was decreased to $< 5 \times 10^{-11}$ Torr after the cryogenic panel was filled with liquid nitrogen.

The substrates were then AES analyzed, resistively heated above 1000°C and reanalyzed, to determine the level and type of surface contamination

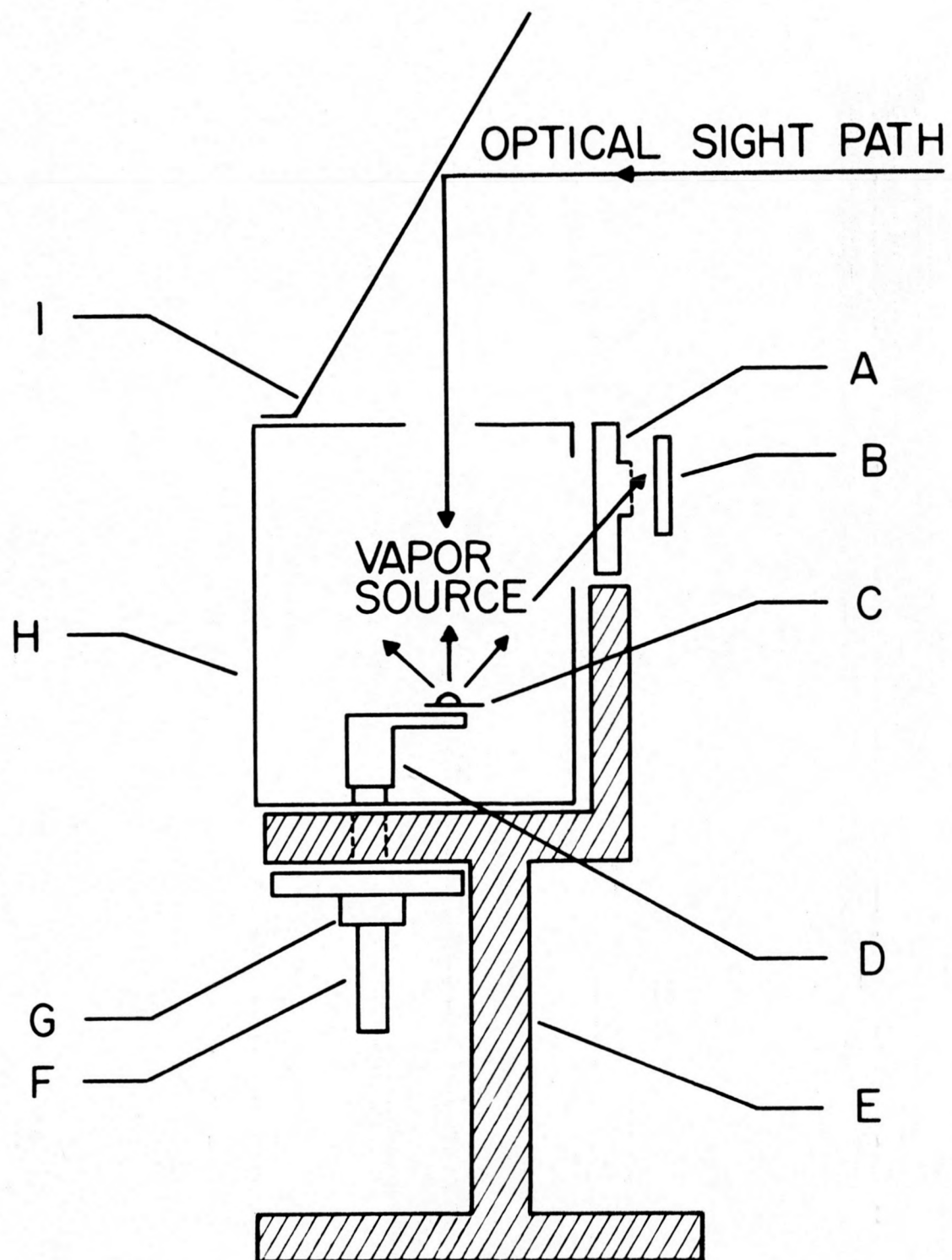


Figure 4. A schematic of the metal evaporation unit for depositing contact electrodes on silicon. Shown is A, the contact electrode pattern mask; B, the substrate; C, the metal source and tungsten boat; D, the tantalum electrode; E, the stainless steel frame; F, the copper electrodes; G, the dual-feedthrough; H, the vapor shield; I, the mirror.

prior to silicon deposition. During deposition the partial pressure of hydrogen rose to 5×10^{-8} to 5×10^{-10} Torr which represented 98% of the total residual gas. The deposition rate of silicon was controlled by the power to the electron beam gun while the substrate temperature was maintained by resistive heating.

After the completion of deposition, the surface was again analyzed by AES. If the experiment required metal electrodes to be placed on the silicon deposit (for electrical characterization studies), they were vapor deposited using the Metal Evaporation Unit.

(b) Specimen Analysis. The analytical techniques and instruments, described below, were employed to fully characterize the substrate and the thin silicon deposit with respect to crystallographic orientation and structure, grain size and surface morphology, thin film composition and electronic properties. To characterize the specimens, x-ray and electron diffraction analysis, AES surface and depth profiling analysis, scanning electron microscopy (SEM) and optical microscopy of the surface and cross sectional topography were employed.

1. Optical and Electron Microscopy. The morphology, grain size, film thickness and structure of the specimens were determined from photomicrographs of the top and edge views obtained using the optical microscope and the SEM.

A cross sectional profile of the specimen was required to provide information on the grain growth at the surface and the silicon thickness. The sample was mounted in Buehlers Transoptic powder, which is a transparent thermoplastic material. The sample was then mechanically polished to reveal the deposit and interface regions. Subsequent chemical etching exposed the

grain structure. Silicon grains as small as 2000 to 3000 \AA thick were observed using these procedures.

2. X-ray and Electron Diffraction Analysis. The Debye-Scherrer camera and the x-ray diffractometer were two techniques employed in this investigation to determine the presence of thin layers of silicide and the orientation of substrates and silicon deposits; e.g. sharp x-ray patterns implied grain sizes greater than 100 \AA .

The SEM, operating in the electron channeling mode, was used to detect crystalline grains greater than one micron in size.

3. Surface Analysis. The AES was the primary in-situ instrument used in this study. In the SSC, the in-situ AES measured the type and level of surface contamination and detected the presence of substrate material which had diffused through the silicon deposit. In a separate facility, AES depth profiles of the samples were made.

4. Electrical Measurements. A current-voltage measurement was made to determine the metal semiconductor (Schottky) barrier height. A bias voltage (V) was placed across the device and the resulting current (I) was measured. A plot of the current density versus voltage was used to calculate the barrier height.

RESULTS AND DISCUSSION

The earlier work in the Ames Laboratory involving silicon deposition on clean metal substrates indicated that the rapid reaction of silicon with the substrate at high temperatures severely restricted the temperature range in which non-reacting deposits could be made. At the same time, a high temperature deposition was desirable to maximize the silicon grain size. During this study silicon was deposited on substrates of tungsten, molybdenum, tantalum and molybdenum disilicide (MoSi_2). A total of nine tungsten and five molybdenum substrates were employed to study the grain growth of silicon from 550°C to above the initial silicide formation temperature. In addition, three tantalum substrates were studied to determine the formation temperature of the silicide and investigate the possibility of silicon growth on the hexagonal TaSi_2 rather than the tetragonal MoSi_2 and WSi_2 . Finally, a total of eleven large grain MoSi_2 wafers were used as substrates to investigate the effects of temperature, oxygen pressure and orientation on the heteroepitaxial growth of silicon.

A. Tungsten Substrates.

Silicon was deposited on a total of nine tungsten substrates to determine the feasibility of growing large grain polycrystalline silicon on ultraclean substrates at low temperature. These substrates were electro-polished to obtain a uniform polished surface. The first substrate 1-01-1 was recrystallized by means of a defocused electron beam in a separate facility to obtain grains that measured between 5 and 20 μm in cross section. All subsequent substrate recrystallization was performed in-situ with

substrate 1-41-1 annealed at 1900°C for 60 min while substrates 1-81-1, 1-81-2, 1-81-3 and 1-91-1 were annealed at 2050 to 2100°C for 1440 min (24 hr) prior to deposition. The details of the anneal procedure are summarized in Table II. In experiment 1-101, a 1700°C recrystallization anneal for 360 min was employed. In that experiment, three metals, tungsten, molybdenum and tantalum were welded to a tantalum ribbon which constituted one substrate assembly. For each deposition three samples were prepared, and in the following discussion 1-101-1W refers to the tungsten substrate, 1-101-1Mo to the molybdenum substrate and 1-101-1Ta to the tantalum substrate all of which were prepared during the deposition on substrate assembly 1-101-1.

For the first two tungsten substrates, 1-01-1 and 1-41-1, the in-situ Auger analysis of the tungsten surface gave nearly identical results of ~1% carbon coverage and 25% oxygen coverage after the anneal. In all subsequent experiments, the AES filaments remained off until the depositions were completed to reduce the possibility of recontamination. The silicon source for the first deposition was 15 ohm-cm, p-type, but this was changed to a 0.008 ohm-cm phosphorus doped n-type silicon ingot in experiment 1-41.

Silicon was deposited on the crystallized tungsten substrates in the temperature range of 550°C and 850°C to promote maximum grain growth with the highest substrate temperature available without silicide formation. These samples were divided into two classes. The first classification included 1-01-1, 1-41-1, 1-81-1, 1-81-2, 1-81-3 and 1-91-1 and are considered a low temperature deposition since no silicide formed. The second classification included 1-101-1W, 1-101-2W and 1-101-3W and silicide formation was present.

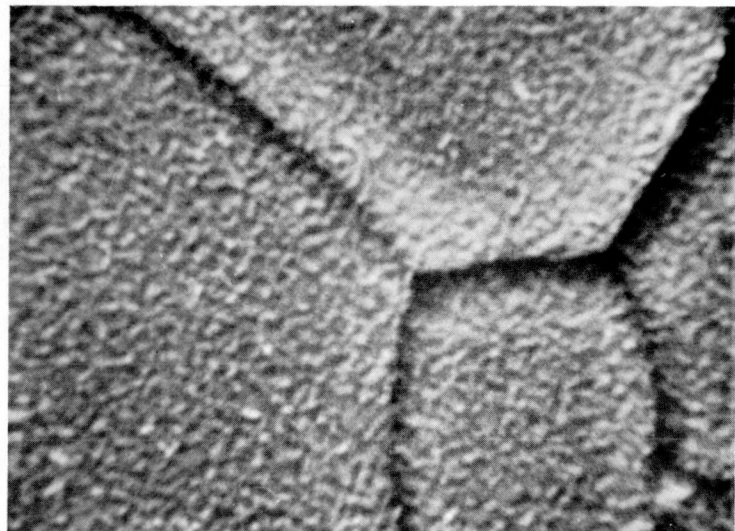
Table II. Experimental conditions for annealing and deposition of silicon on tungsten substrates.

Substrate No.	Annealing Temp. (°C)	Time at Temp. (min.)	Pressure Max. (Torr)	Deposition Temp. (°C)	Deposition Time (min.)	Deposition Rate (Å/min.)	Press. During Deposit (Torr)	Max. Thickness (μm)
1-01-1	1100	60	---	550	460	75	---	3.5
1-41-1	1100	60	8×10^{-9}	550	300	150	---	4.5
1-81-1	2050	1440	6×10^{-8}	450 560	305 295	160	1.2×10^{-7}	9.5
1-81-2	2050	1440	1.3×10^{-8}	560	600	150	5.2×10^{-9}	9.0
1-81-3	2050	1440	3×10^{-8}	590	600	330	6×10^{-9}	20.0
1-91-1	2100	1440	2.5×10^{-8}	630	600	630	1.6×10^{-7}	38.0
1-101-3W	1700 850 750 1400	360 750 60	1×10^{-8}	670	360	~150	2.8×10^{-9}	~5.5
1-101-2W	1700 850 1400	360 900 60	1.4×10^{-8}	750	360	~250	5.5×10^{-9}	~9.0
1-101-1W	1700 850 1400	360 900 60	1.2×10^{-8}	850	360	~250	8×10^{-8}	~9.0

(a) Silicon Deposition Below 650°C. In this first group in which silicon was deposited on tungsten between 550°C and 630°C, there were little apparent differences in the surface morphology and orientation of the deposits. The top and edge view of sample 1-01-1, deposited at 550°C, is shown in Figure 5(a) and (b), and is representative of the silicon grain structure where the grain size did not exceed 3000 Å in cross section. The orientation of this deposit was determined as {110} by x-ray analysis. For experiment 1-41, the silicon source was changed to the high phosphorus doped ingot, and substrates were recrystallized *in-situ*, but no change in morphology or orientation was noted. for 1-41-1. By increasing the deposition temperature to 560° for 1-81-2, 590°C for 1-81-3 and 630°C for 1-91-1, it was hoped the silicon grain size could be increased. However, the photomicrographs in Figure 6(a), (b) and (c) show no significant improvement in the grain size for 1-81-2, 1-81-3 and 1-91-1 respectively. The orientation of the silicon deposits was {110} but minor planes of {111} and {311} were also detected by x-ray analysis. The details of this x-ray analysis are summarized in Table III. In view of the surface morphology described in the photomicrograph in Figure 5(a), 6(a), (b) and (c), it was not surprising that psuedo-Kikuchi patterns were not obtained when these deposits were examined by electron channeling techniques. Figure 5(a) shows a fine grain silicon layer on tungsten substrate grains. From optical microscopy and from electron channeling patterns, we conclude that the deposited layer only replicates the tungsten substrate.

(b) Silicon Deposition Above 650°C. For the second series of tungsten substrates, the deposition temperatures, T_D , were 850°C for 1-101-1W, 750°C for 1-101-2W, and 670°C for 1-101-3W. The effects of increased temperature are very apparent as one examines Figures 6(d), (e) and (f) for samples

a)



b)

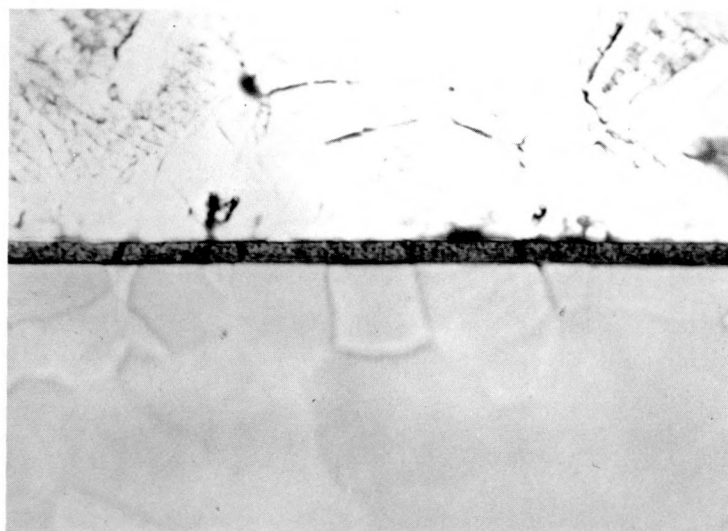


Figure 5. SEM and optical photomicrographs of 1-01-1 showing a surface and edge view of the fine grain {110} silicon deposited on {100} tungsten. (a) SEM photomicrograph taken at 8800X showing the replication of silicon on the substrate. (b) An optical photomicrograph taken at 1400X showing the fine grain silicon after etching.

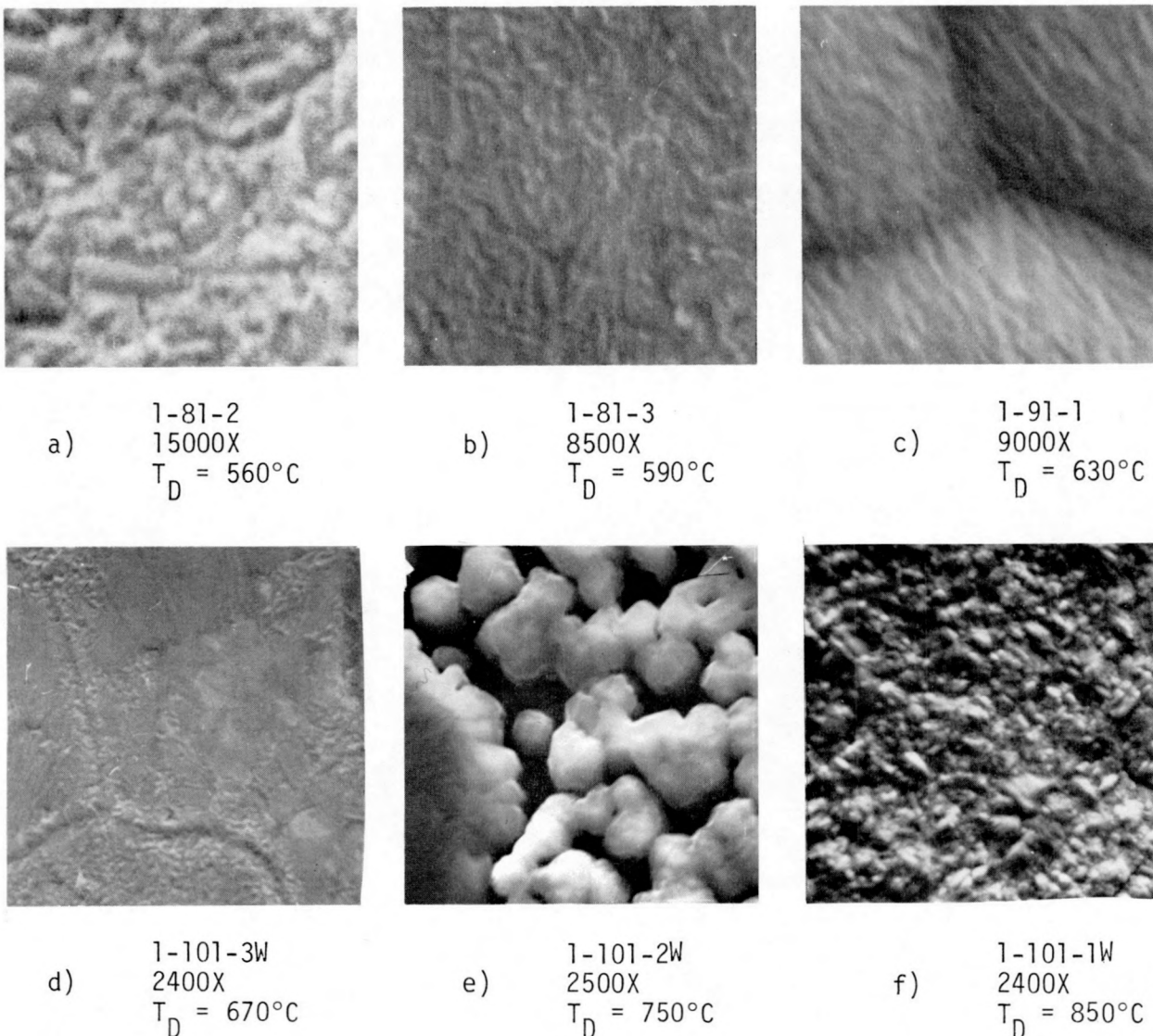


Figure 6. SEM photomicrographs of the surface topography of silicon vacuum evaporated on tungsten substrates where the deposition temperature, T_D , was between $560^\circ C$ and $850^\circ C$.

Table III. Summary of the results for x-ray analysis and grain size measurements for tungsten substrates.

Substrate No.	Primary Substrate Orientation	Substrate Grain Size (μm)	Silicon Orientation		Silicon Grain Size (μm)
			Primary	Secondary	
1-01-1	{100}	5-20	{110}	---	0.3
1-41-1	{100}	5-60	{110}	---	0.3
1-81-1	{100}	5-90	{110}	{111} {311}	0.3
1-81-2	{100}	5-90	{110}	{111}	0.3
1-81-3	{100}	5-90	{110}	{111} {311}	0.3
1-91-1	{100}	5-90	{110}	{311}	0.3
1-101-3W *	{100}	5-90	silicide, {111}, {110}	{100} {311}	0.3-30
1-101-2W	{100}	5-90	silicide	---	---
1-101-1W	{100}	5-90	silicide	---	---

* Channeling obtained from this substrate.

1-101-3W, 1-101-2W and 1-101-1W respectively.

Sample 1-101-3W, shown in Figure 6(d), was prepared at $T_D = 670^\circ\text{C}$ and the resulting deposit possessed two distinct morphologies. The first was similar to those described for substrates prepared at $T_D \leq 630^\circ\text{C}$, that is, fine grain crystallites measuring $\sim 3000 \text{ \AA}$ across. The second type structure, which was generally greater than $30 \mu\text{m}$ in lateral extent, was smooth, flat and produced poor quality pseudo-Kikuchi patterns when examined with electron channeling. In addition to the $\{100\}$ tungsten substrate, the x-ray detected the presence of planes of $\{111\}$ and $\{110\}$ silicon. No metal was detected on the surface with the in-situ AES, but approximately 1% phosphorus and 1% sulfur coverage was determined to be on the surface.

The next sample, 1-101-2W, was prepared by depositing silicon on a substrate held at 750°C . Although no tungsten was detected at the surface of this sample, $\sim 2\%$ phosphorus coverage and a total of $\sim 1\%$ coverage for sulfur, oxygen and carbon was found by in-situ Auger analysis. The grains produced by this deposition, shown in Figure 6(e), were clusters that measured 2.5 to $10 \mu\text{m}$ in cross section. The x-ray results indicated that both silicon and tungsten silicide were present. Thus, a finite thickness of silicon remained unreacted on the tungsten silicide base layer. The size of these grains was well within the capability of the channeling technique but no patterns could be obtained.

For the final sample in the series, 1-101-1W, silicon was deposited at a temperature of 850°C and reacted to form WSi_2 . Figure 6(f) shows the granular morphology of the deposited film that in-situ analysis confirmed as WSi_2 . These structures measured $\sim 2 \mu\text{m}$ across.

To summarize these results, we have deposited silicon on recrystallized

tungsten with {100} orientation. Polycrystalline silicon grains measuring 3000 Å in cross section grew in {110} orientation between 550°C and 630°C without the formation of a silicide. We have attributed the suppression of the silicide at the higher deposition temperature to the presence of phosphorus. At 670°C, silicon grew on tungsten in both the {111} and {110} planes. The surface had flat regions on the silicon deposit that measured 30 μm in cross section. These were examined by electron diffraction techniques and weak electron channeling patterns were obtained. This channeling result implies these areas are composed of smaller grains measuring only a few microns in cross section. An intermediate condition was obtained at 750°C in which the silicon arrival rate was slightly greater than the silicide formation rate. The resulting deposit consisted of silicide grains that were overlayed with a fine-grained silicon. At 850°C, all of the silicon reacted with the substrate to form WSi_2 .

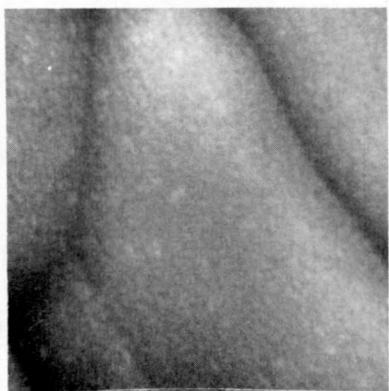
B. Molybdenum Substrates.

A total of five molybdenum substrates, 1-01-2, 1-01-3, 1-01-1Mo, 1-101-2Mo, 1-101-3Mo, were prepared within the temperature range of 550°C to 850°C. The first two substrates, 1-01-2 and 1-01-3, were recrystallized in vacuum for 410 min at 1100°C prior to loading in the SSC. These substrates possessed grains 10-60 μm in cross section with the orientation of the grains in the {100} plane but with some {211} planes also present. In the SSC the substrates were annealed to 1000°C for 60 min to completely remove the surface contamination. Auger analysis after the anneal revealed that the surface still contained 1% carbon and 10% oxygen. The three remaining substrates were annealed in-situ at 1700°C for 360 min to produce

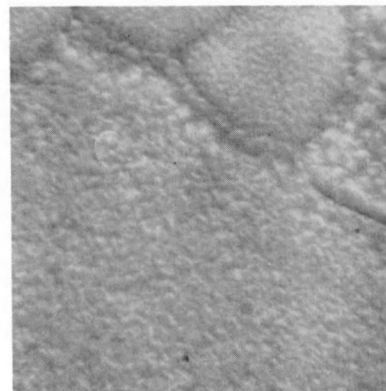
molybdenum grains between 5 and 60 μm in cross section and having a $\{100\}$ orientation. The Auger analysis was not performed to reduce the risk of contamination by the degassing of AES filaments.

(a) Silicon Deposition Below 670°C. Substrate 1-01-2 was maintained at 550°C while silicon was deposited at a rate of 300 $\text{\AA}/\text{min}$ for 100 min. To enhance silicon grain growth, T_D was raised to 650°C for the deposition on substrate 1-01-3. After cooling the samples, the in-situ Auger analysis of the two samples indicated that a reaction of molybdenum and silicon occurred only in 1-01-3. The surface morphology for sample 1-01-2, shown in Figure 7(a), was similar to tungsten substrate 1-01-1. The x-ray diffraction analysis indicated the silicon on 1-01-2 was crystalline with an orientation of $\{110\}$. Since electron channeling was not obtained, the silicon film was considered polycrystalline with crystallites $\sim 2000 \text{\AA}$ across. An Auger depth profile of 1-01-2 revealed that the interface between silicon and molybdenum was sharply defined, indicating little or no diffusion.

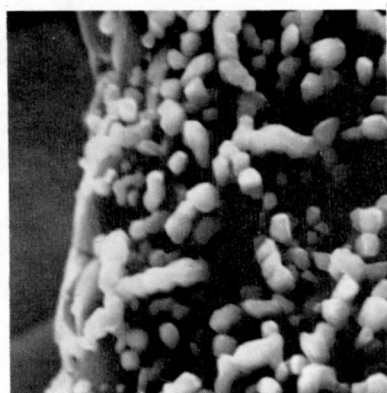
A series of three depositions near and above the silicide formation temperature were made to test the effect of phosphorus in silicon on retarding silicide growth. Substrate 1-101-3Mo was a repetition of 1-01-3. Silicon was deposited at 670°C for 360 min on 1-101-3Mo; however the resulting film, shown in Figure 7(b), was closer to 1-01-2 in structure than 1-01-3. The silicon grains were $\sim 2000 \text{\AA}$ in cross section, and the layer only replicated the substrate grains. The surface was exclusively silicon with only $\sim 1\%$ phosphorus and $\sim 1\%$ sulfur coverage as determined by in-situ AES analysis. The x-ray analysis determined that the silicon orientation was predominantly $\{110\}$ with the $\{111\}$ and $\{311\}$ planes also present.



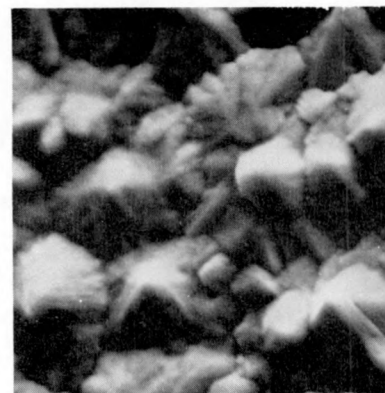
a) 1-101-2
9000X
 $T_D = 550^\circ\text{C}$



b) 1-101-3Mo
2400X
 $T_D = 670^\circ\text{C}$



c) 1-101-2Mo
2400X
 $T_D = 750^\circ\text{C}$



d) 1-101-1Mo
2400X
 $T_D = 850^\circ\text{C}$

Figure 7. SEM photomicrographs of the surface topography of silicon deposited on molybdenum substrates at deposition temperatures, T_D , (a) 550°C, (b) 670°C, (c) 750°C and (d) 850°C.

(b) Silicon Deposited Above 670°C. By increasing the deposition temperature to 750°C for sample 1-101-2Mo, a distinctly different surface morphology shown in Figure 7(c) was produced. These "finger" like structures were $\sim 10 \mu\text{m}$ long and $\sim 1 \mu\text{m}$ in diameter. Although silicon and not molybdenum was detected on the surface of this deposit with the in-situ AES, x-ray analysis confirmed the presence of molybdenum silicides beneath the surface layer of silicon. In addition to the silicon there was $\sim 2\%$ phosphorus coverage of this surface. The final molybdenum substrate in this group was prepared by depositing silicon at 850°C for 360 min. The resulting film was MoSi_2 , and it is pictured in Figure 7(d) which shows its characteristic "hillock" structure. The in-situ Auger analysis revealed that 98% of the surface coverage was MoSi_2 with the balance composed of oxygen, carbon and sulfur. Table IV contains a summary of deposition and characterization data for the five molybdenum substrates.

To summarize, silicon deposited on recrystallized {100} molybdenum grows with {110} planes. With the phosphorus doped silicon source, the deposition temperature was increased from 550°C to 670°C without silicide formation. At 750°C, silicides were formed but the growth of these silicides proceeded at a rate lower than the deposition rate of silicon. As a result, a layer of fine grain silicon covered the silicide grains. When silicon was deposited at 850°C, MoSi_2 was quickly formed.

C. Tantalum Substrates.

A surprising discovery was made when some of the silicon deposit was analyzed on the tantalum envelope surrounding the silicon substrate used in experiment 1-41-2, in which silicon was deposited on a single crystal wafer

Table IV. Experimental conditions and results for silicon deposited on molybdenum.

Substrate No.	Deposition Temperature (°C)	Deposition Rate (Å/min)	Thickness of Deposit (μm)	Substrate Grain Size (μm)	Predominant Substrate Orientation	Silicon Grain Orientation	Silicon Grain Size (μm)
1-01-2	550	300	3	10-60	{100}	{110}	0.2
1-01-3	650	300	3	10-60	{100}	silicide	silicide
1-101-3Mo	670	~150	5.5	5-60	{100}	{110}	0.2
1-101-2Mo	750	~250	9.0	5-60	{100}	silicide	---
1-101-1Mo	850	~250	9.0	5-60	{100}	silicide	---

of silicon. Even though the temperature of the tantalum envelope was probably higher than the 800°C measured at the silicon substrate, no tantalum Auger signal could be detected on the surface of the silicon deposit. Instead only silicon and phosphorus were found. Subsequent analysis by SEM, electron microprobe, AES depth profiles and x-ray analysis revealed that the silicon, nearly five microns thick, covered over 90% of the surface. Beneath these silicon crystals there was a uniform two micron thick layer of $TaSi_2$. A top view of this sample is shown in Figure 8(a) and an edge view is shown in Figure 8(b). Portions of the silicon layer were easily removed and an Auger depth profile through the $TaSi_2/Ta$ interface (1% depth resolution) put an upper limit of less than one monolayer of TaP at the interface. This result ruled out the formation of a TaP diffusion barrier at the $TaSi_2/Ta$ interface. It may be that the phosphorus was uniformly distributed throughout the $TaSi_2$ layer (at a level less than 200 ppma) or in the grain boundaries thereby limiting the diffusion of silicon to the $TaSi_2$, which is known to be the rate limiting step in the formation of $TaSi_2$. In any case, it appears that the presence of phosphorus in the silicon source may significantly suppress the growth rate of $TaSi_2$ at 800°C, by a mechanism not presently understood.

It should be recalled that little effect due to phosphorus doping of the silicon source was evident in the silicon grain structure of the tungsten substrate (1-41-1) deposited at 550°C. Analysis of the tantalum envelopes used in experiment 1-61, where their temperatures were above 1100°C, revealed no phosphorus and complete conversion of the silicon deposit to $TaSi_2$. Evidently at these higher temperatures the effectiveness of a phosphorus doped silicon source is lost, probably because of the much higher

1-41-2

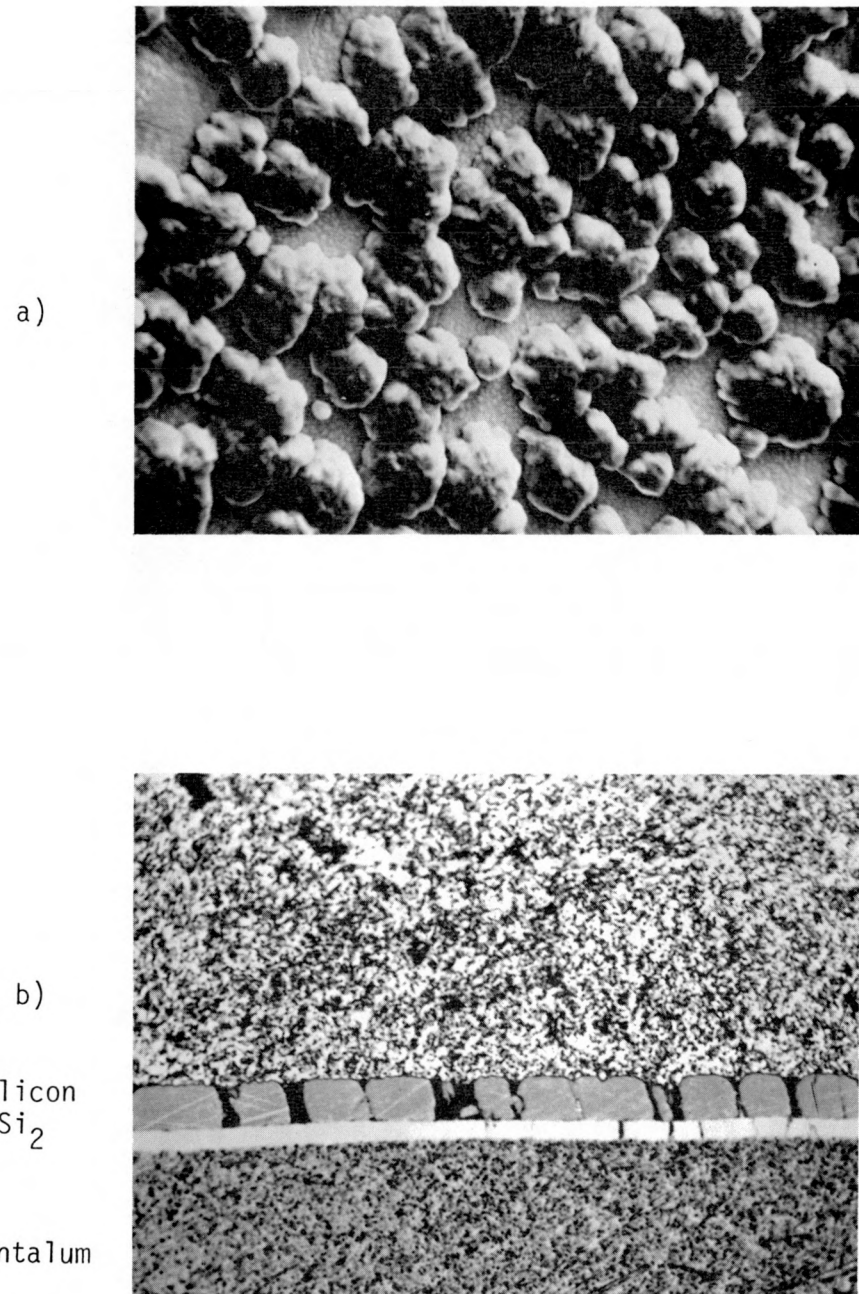
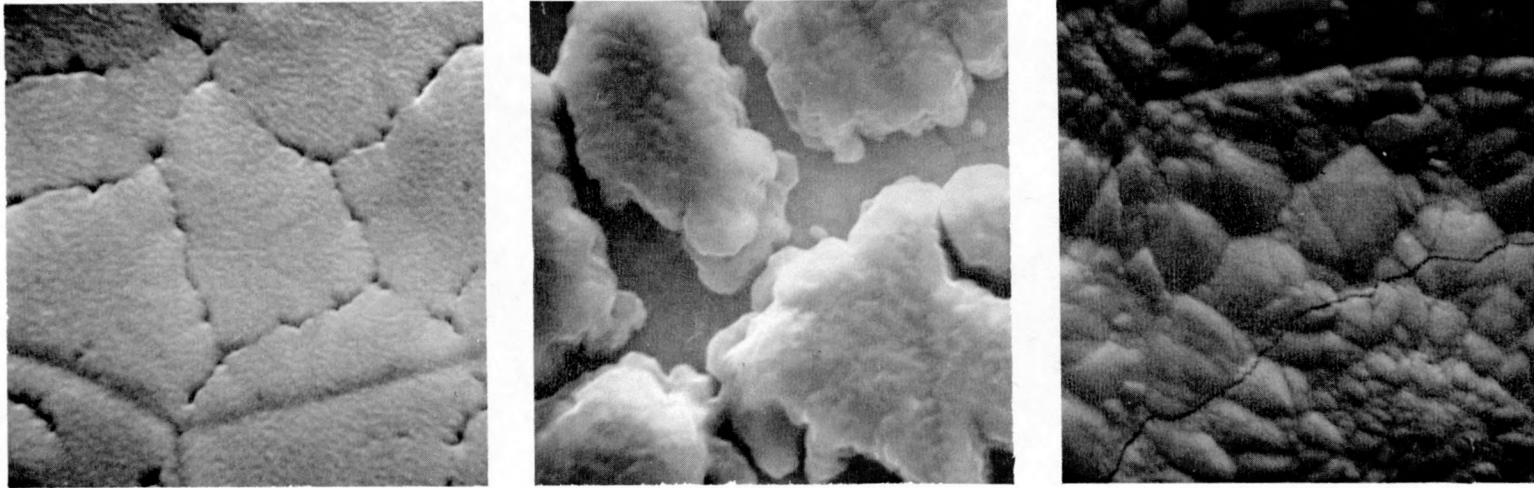


Figure 8. SEM photomicrograph of the surface and an optical photomicrograph of the cross sectional profile of silicon deposited on tantalum in experiment 1-41-2 (a) SEM micrograph taken at 1200X showing crystalline.

rate of evaporation of phosphorus from the hotter tantalum envelopes. These results combined with the successful silicon growth at 800°C reported above suggest that there may be an optimum temperature at which the beneficial effects of the co-evaporating phosphorus has a maximum effect. To investigate this phenomena, the following series of silicon depositions on tantalum was undertaken with substrate temperatures at 670, 750 and 850°C.

The three tantalum substrates used in this experiment, 1-101-1Ta, 1-101-2Ta and 1-101-3Ta were annealed in-situ for 360 min at 1700°C to produce grains of tantalum that exceeded 50 μm in cross section. These grains recrystallized in a preferred orientation of {211} and {111}. Silicon was deposited on substrate 1-101-3Ta for 360 min at 670°C. The photomicrograph of the resulting deposition, Figure 9(a), shows a surface with fine grain structure, but this layer had begun to segregate into islands $\sim 15 \mu\text{m}$ in cross section. The composition of this deposit was 98% silicon with $\sim 1\%$ phosphorus and $\sim 1\%$ sulfur coverage as determined by in-situ Auger analysis. Silicon was deposited on 1-101-2Ta for 360 min at 750°C. While viewing the surface of 1-101-2Ta in Figure 9(b), it was apparent that the segregation noted in Figure 9(a) had progressed. The island-like structures shown in Figure 9(b) are 20 μm across and have exposed the substrate. Thus, the in-situ Auger analysis of this layer produced $\sim 1\%$ tantalum coverage in addition to $\sim 2\%$ phosphorus coverage and $\sim 1\%$ coverage for carbon, oxygen and sulfur. This deposit has proved to be very unstable, and extreme caution was required while handling it to prevent the deposit from flaking off. At the deposition temperature of 850°C, silicon was evaporated for 360 min on substrate 1-101-1Ta. The in-situ AES detected the formation of TaSi_2 as well as $\sim 2\%$ coverage of the surface with sulfur, oxygen and carbon. The



a

b

c

Figure 9. SEM photomicrographs of the surface topography of silicon deposited on tantalum as a function of deposition temperatures, T_D . (a) Sample 1-101-3Ta, $T_D = 670^\circ\text{C}$, magnification 2400X. (b) Sample 1-101-2Ta, $T_D = 750^\circ\text{C}$, magnification 2400X. (c) Sample 1-101-1Ta, $T_D = 850^\circ\text{C}$, magnification 2400X.

morphology of $TaSi_2$ is described as "rosette" like and is shown in Figure 9(c). None of the above deposits showed signs of crystallinity by channeling techniques. Table V summarizes the results and experimental conditions for silicon deposited on tantalum substrates.

To summarize the above result, silicon deposited at 670°C, produced a fine grain deposit that was beginning to segregate into regions measuring 15 μm across. The silicon growth at this temperature is attributed to the phosphorus in the silicon source. The second deposition, 1-101-2Ta, was made at 750°C, and the deposited silicon formed island-like structures that resembled the structure on the tantalum envelope in experiment 1-41-2 in which silicon was deposited on a silicon substrate. The major difference between these experiments was that 1-41-2 produced crystalline grains and 1-101-2Ta did not. Also, the deposit on substrate 1-101-2Ta was not mechanically stable and flaked off the substrate. This instability suggests that the silicon merely coated the substrate and did not diffuse into the metal. If this is true, the phosphorus could have inhibited interdiffusion. At 850°C, $TaSi_2$ was formed as rapidly as the silicon was deposited on tantalum.

D. Silicides.

Two approaches to the silicide formation problem were suggested by the previous results and by the kinetics of the silicide reaction. The growth of a silicide layer is diffusion-limited, but it is not clear whether the rate limiting step is bulk or grain boundary diffusion. If it is bulk diffusion, then a thicker silicide layer should reduce the reaction rate. If it is grain boundary diffusion, then large grain silicide should be used. Two

Table V. Experimental conditions and results for silicon deposited on tantalum substrates.

Substrate No.	Deposition Temperature (°C)	Deposition Rate (Å/min)	Thickness of Deposit (μm)	Substrate Grain Size (μm)	Predominant Substrate Orientation	Silicon Grain Orientation	Silicon Grain Size (μm)
1-101-3Ta	670	~ 150	5.5	~50	{211} {111}	{111} {110}	~0.3
1-101-2Ta	750	~ 250	9.0	~50	{211} {111}	not detected	~0.3
1-101-1Ta	850	~ 250	9.0	~50	{211} {111}	silicide	-----

types of experiments were performed. The first was the growth of a thick MoSi_2 layer on a clean molybdenum substrate to determine whether this thick silicide layer would reduce silicide growth during silicon deposition at temperatures above 650°C. The second type of experiment utilized the polycrystalline MoSi_2 substrate that eliminated the silicide reaction because the free metal was removed. In the second type of experiment, large silicon grains were grown on polycrystalline MoSi_2 as a function of temperature and the oxygen partial pressure.

(a) Silicon Deposition on MoSi_2 Grown on Molybdenum. Five molybdenum substrates, 1-11-1, 1-11-2, 1-11-3, 1-91-2 and 1-91-3, were used to study rapid high temperature silicide formation. The first three substrates, 130 μm thick, were electropolished and then annealed in a separate furnace for 930 min at 1100°C under a pressure of 5×10^{-6} Torr. The resulting molybdenum grains measured 10 to 60 μm across. The substrates were attached to heavy tantalum electrodes so that a large temperature gradient could be obtained across the length of the substrate. A thermocouple attached at the center of the substrate was used to first determine a reference temperature after which an optical pyrometer was used to determine the temperature gradient. This arrangement followed an evaluation of the silicide grain morphology as a function of deposition temperature.

Silicon was deposited on molybdenum substrate 1-11-1 for 600 minutes with the substrate center maintained at 1215°C, while the ends of the substrates were at $\sim 1080^\circ\text{C}$. After cooling the substrate, in-situ Auger analysis indicated MoSi_2 on the surface. Substrate 1-11-2 was held at a temperature of 1000°C at its center during silicon deposition. The temperatures near the ends of the substrate were about 875°C. The in-situ Auger analysis

of this substrate also indicated the formation of MoSi_2 as observed for 1-11-1 above.

The silicide growth conditions for the third substrate, 1-11-3, were the same as for 1-11-1. The in-situ Auger analysis of the surface after the 1200°C silicon deposit again indicated MoSi_2 . The temperature of the substrate with MoSi_2 layer was then held at 700°C for 500 minutes to deposit a 5 μm layer of silicon. After this deposition, the Auger analysis indicated interdiffusion of the silicon and molybdenum at the center although near the cooler ends only silicon was found. The x-ray analysis of the three samples after removal from the vacuum system showed the presence of the two silicide phases, Mo_5Si_3 and MoSi_2 . Electron channeling and optical photomicrographs were used to determine the size of the surface MoSi_2 grains. The results of these measurements and the deposition data for these three substrates are shown in Table VI.

The substrates were edge mounted to obtain a better view of the morphology of the deposited films. Figure 10 shows photomicrographs of the cross sections in polarized light and with normal illumination after etching for the center of three samples. Sample 1-11-1 had two distinct layers on the molybdenum surface. First there is a layer 10 to 15 μm thick next to the molybdenum which has been identified as Mo_5Si_3 . On top of this layer is an equally thick layer of MoSi_2 . The relatively large columnar grains of the MoSi_2 can be seen in Figure 10(a) and (d).

In Figure 10(b) and (c) of sample 1-11-2, which was prepared at 1000°C, the layer of Mo_5Si_3 is much thinner; yet, a 10 μm thick layer of MoSi_2 was found. The interpretation of the photo of 1-11-3 is complicated since the silicon deposited at 700°C reacted with the MoSi_2 layer forming a fine grain region. Near the end of the substrate, where the temperature was

Table VI. Experimental conditions and results for Experiment 1-11.

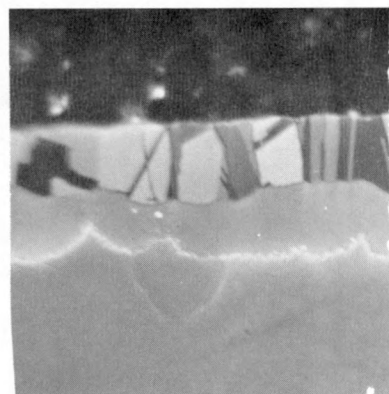
Substrate No.	Silicon Deposition Temp. (°C)	Silicide Phases Found	2nd Si Deposition	MoSi ₂ Grain Size (μm)
	center/end			center/end
1-11-1	1215/1080	MoSi ₂ , Mo ₅ Si ₃		10/10
1-11-2	1000/875	MoSi ₂ , Mo ₅ Si ₃		10/7
1-11-3	1200/1010	MoSi ₂ , Mo ₅ Si ₃	700	10/1

1-11-1

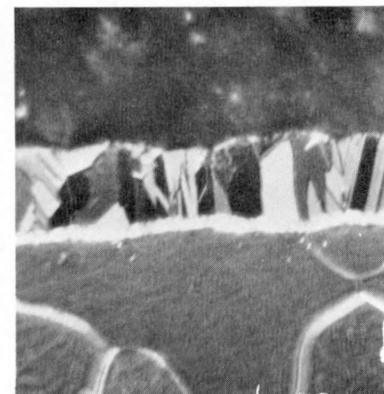
1-11-2

1-11-3

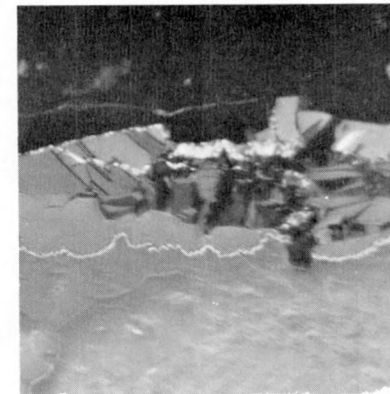
Polarized



a

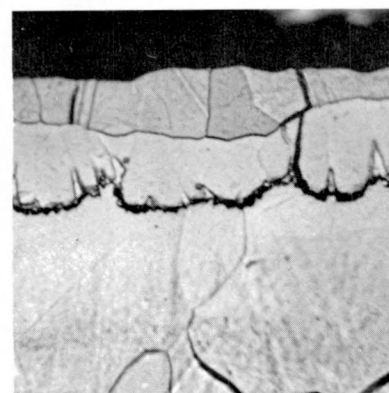


b

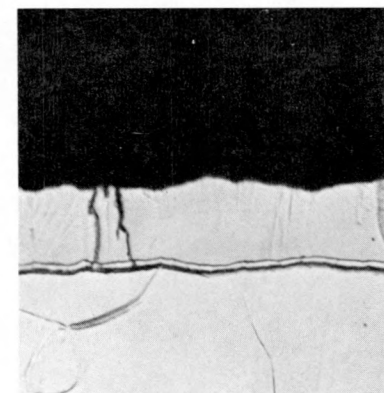


c

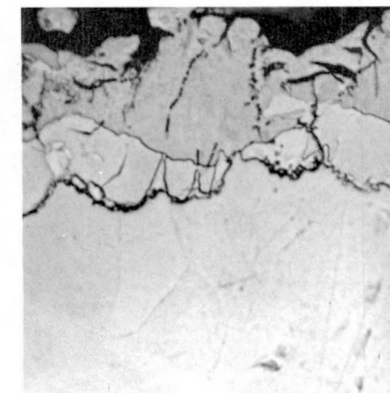
Normal



d



e



f

Figure 10. Optical photomicrographs of the cross sectional profile of samples 1-11-1, 1-11-2 and 1-11-3. At 1000X, these micrographs show the MoSi_2 and Mo_5Si_3 layers on the molybdenum substrate. Pictures a, b, and c were photographed using polarized light while d, e, and f were photographed after etching with normal illumination

lower, a layer of silicon was maintained on top of the large grain MoSi_2 as shown in Figure 11.

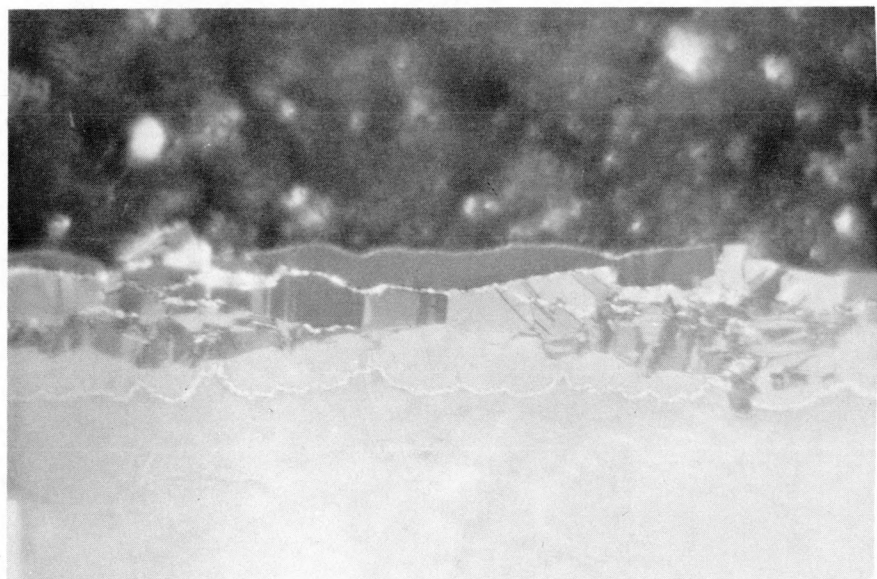
In a continuation of this study, the large grain molybdenum substrates were employed for experiment 1-91-2 and 1-91-3. By depositing silicon at 1400°C on molybdenum having a grain size of $\sim 1 \text{ cm}^2$, it was believed that the MoSi_2 grain growth would be enhanced. The molybdenum substrates 1-91-2 and 1-91-3 with a thickness of 210 μm and 180 μm respectively were annealed for 180 min at 1400°C in-situ at a maximum pressure of 1×10^{-8} Torr. Silicon was deposited on 1-91-2 at 1410°C for 300 min and on 1-91-3 at 1440°C for 300 min. After the deposition on 1-91-3, the substrate temperature was reduced to 800°C and the substrate was translated 0.5 cm for a second 300 min deposition. Thus, on sample 1-91-3, three deposition regions were obtained. In comparing the 1400°C deposition regions for 1-91-2 and 1-91-3, there was little apparent difference in the surface morphology. The in-situ Auger analysis indicated that Mo_2Si was present at the surface of each 1400°C deposit. An SEM photomicrograph of the 1400°C deposit of 1-91-3 is given in Figure 12(a). In Figure 12(b), silicon deposited at 800°C on top of the deposit made at 1400°C is shown and the surface concentration was determined to be MoSi by in-situ Auger analysis. Silicon evaporated at 800°C directly on the large grained molybdenum substrate, shown in Figure 12(c), formed MoSi_2 . Table VII is a summary of conditions and results of silicon deposited on molybdenum substrates 1-91-2 and 1-91-3.

Under the conditions investigated, it appeared that silicon deposited at 700°C reacted completely with the grown silicide layer preventing silicon growth. The attempts to produce silicides by reaction of silicon at its melting point with large grain molybdenum did not significantly increase the

1-11-3

a)

Polarized

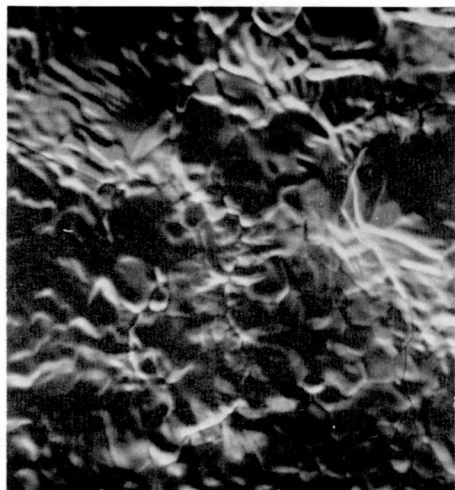


b)

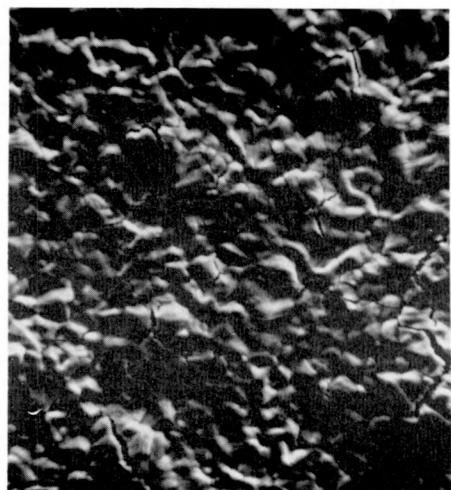
Normal



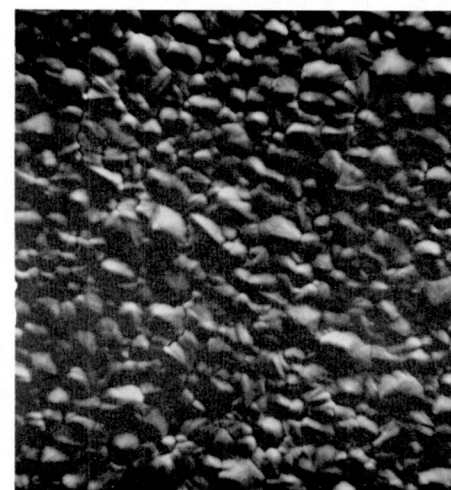
Figure 11. Optical photomicrograph of a cross sectional profile of silicon deposited near the end of sample 1-11-3. (a) Micrograph taken at 1000X under polarized light. (b) Micrograph taken at 1000X after etching showing fine grains of silicon.



a



b



c

Figure 12. SEM photomicrographs of the surface of Sample 1-91-3 showing silicon deposited on large grain molybdenum at elevated temperature. (a) Silicon deposited at substrate temperature, $T_D = 1400^\circ\text{C}$, magnification 900X. (b) Silicon deposited at $T_D = 800^\circ\text{C}$ on the layer shown in (a), magnification 900X. (c) Silicon deposited on large grain molybdenum at $T_D = 800^\circ\text{C}$, magnification 900X.

Table VII. Experimental conditions and results of silicon deposited on molybdenum in Experiment 1-91.

Substrate No.	1st Silicon Deposition Temp. (°C)	2nd Silicon Deposition Temp. (°C)	Silicide Phase on the Surface*
1-91-2	1410	---	Mo_2Si
1-91-3	1440	---	Mo_2Si
	1440	800	MoSi
		800	MoSi_2

*In-situ AES analysis.

silicide grain size. A subsequent silicon deposition at 800°C on this silicide layer was unsuccessful since silicon reacted to form MoSi. From these results we cannot determine whether the rate of silicide formation was governed by silicon diffusion along grain boundaries or by the high reactivity rate at these temperatures. Silicides grown at high temperatures were not found to be an inhibiting layer to further silicide formation at the lower temperature.

(b) Silicon Deposition on Large Grain Polycrystalline MoSi₂. In the next series of experiments, large grain polycrystalline MoSi₂ substrates were used which eliminated the consumption of silicon by the free metal. The problem then becomes a study of the effect of temperature, background gas and orientation on the growth of silicon on MoSi₂.

In our first experiment, MoSi₂ substrates 1-31-1 and 1-31-3 were mounted in the SSC. Substrate 1-31-1 was heated to 1300°C for 90 minutes, after which the temperature was lowered to 1000°C and silicon from the p-type ingot was deposited at 5000 Å/min for 20 minutes. The in-situ Auger analysis showed only silicon on the surface of the nominal 10 µm silicon layer. Subsequent electron channeling and topography studies in the SEM revealed 5 µm diameter silicon grains.

The second substrate, 1-31-3, was also heated to 1300°C for 90 minutes and silicon was deposited at 1200°C at a rate of 250 Å/min. The in-situ Auger analysis of this sample also indicated only silicon on the surface. After removal from the vacuum chamber, topography and electron channeling studies with the SEM indicated 20 to 25 µm diameter silicon grains. The x-ray measurements of these large grains revealed that they were oriented predominantly in the {111} and {110} direction.

The results for these two substrates demonstrate the feasibility of growing large grain silicon on MoSi_2 substrates. The next step in the study was to evaluate the effects of the partial pressure of oxygen on the grain size of the deposited silicon.

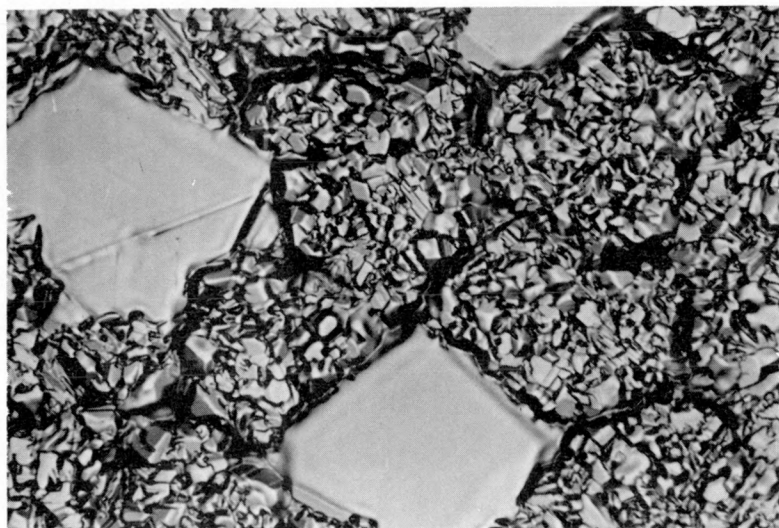
1. Effects of Oxygen Partial Pressure. Three MoSi_2 substrates numbered 1-61-1, 1-61-2 and 1-61-3 were mounted in tantalum heating ovens. Two major changes from the 1-31 depositions were made for these substrates. The p-type silicon ingot was replaced by a phosphorus doped n-type silicon ingot in the new mold assembly described in the experimental section. Also, the metallization unit was installed in the vacuum system and used to evaporate gold contacts on the silicon films. Except for the oxygen partial pressure, the experimental conditions were maintained nearly identical for all three substrates. The silicon deposition temperature was 1100°C .

Silicon was deposited on substrate 1-61-3 with the lowest oxygen partial pressure (1.8×10^{-12} Torr) that could be obtained. Successively greater oxygen partial pressures were introduced for the other two substrates. Data for the three 1-61 depositions are listed in Table VIII.

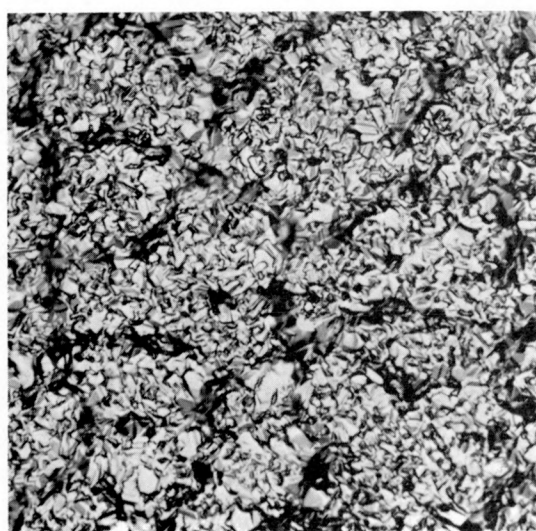
Figures 13(a), (b), and (c) show the top views of samples 1-61-3, 1-61-2, and 1-61-1, respectively. There is little difference in the morphology of samples prepared under an oxygen partial pressure of 1×10^{-8} Torr for 1-61-1 and 1×10^{-10} Torr for 1-61-2. Both have crystalline silicon grains, as confirmed by electron channeling, from 2 to $8 \mu\text{m}$ in cross section which were grouped into clusters ranging from 20 to $40 \mu\text{m}$ across. The silicon morphology of 1-61-3, prepared in the base pressure environment of the SSC (oxygen partial pressure of 1.8×10^{-12} Torr) is quite different. Silicon grains as large as $60 \mu\text{m}$ are evident in Figure 13(a). In other

Table VIII. Experimental conditions and results for silicon deposition on MoSi_2 .

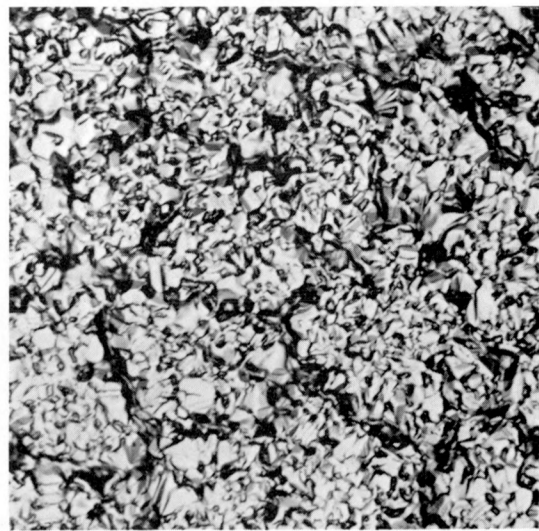
Sample No.	Anneal Time min.	Anneal Temp. °C	Max. Anneal Pressure Torr	Silicon				Pressure of O_2 During Si Deposition Torr
				Deposition Rate A/min	Deposition Temp. °C	Film Thickness μm	Grain Size μm	
1-61-3	80	1200	5×10^{-8}	950	1100	9.5	20-200	1.8×10^{-12}
	100	1100						
1-61-2	180	1100	4.0×10^{-8}	800	1100	8.0	2-8	1.0×10^{-10}
1-61-1	180	1100	1.7×10^{-8}	730	1100	8.0	2-8	1.0×10^{-8}
1-71-1	200	1050	3.3×10^{-9}	1000	950	10	2-80	4.7×10^{-13}
1-71-2	200	1050	4.1×10^{-9}	1200	800	12	<1-50	4.5×10^{-13}
1-71-3	200	1050	3.0×10^{-8}	500	650	5	<1	4.0×10^{-13}
1-111-1	180	1100	4×10^{-9}	215	800	6.4	2-20	6.1×10^{-13}
1-111-2	180	1100	8×10^{-11}	180	800	1.8	2-80	1.6×10^{-13}
1-111-3	180	1075	8×10^{-10}	280	800	2.8	2-80	1.6×10^{-8}



a



b



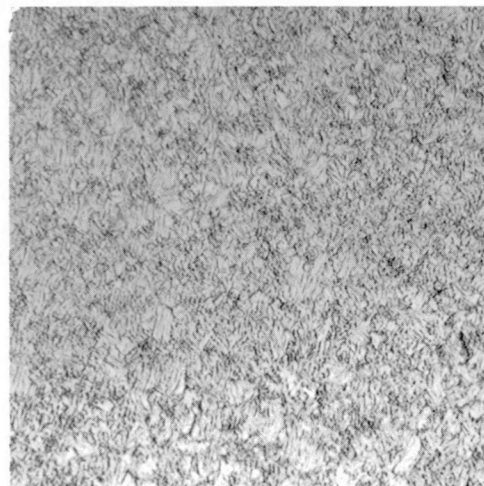
c

Figure 13. Optical photomicrographs taken at 500X of silicon deposited on 1-61-3, 1-61-2, 1-61-1 at a substrate temperature, $T_D = 1100^\circ\text{C}$. (a) Sample 1-61-3 has an oxygen partial pressure, P_{O_2} , during deposition of 1.8×10^{-12} Torr. (b) Sample 1-61-2 deposited at $P_{O_2} = 1.0 \times 10^{-10}$ Torr. (c) Sample 1-61-1 deposited at $P_{O_2} = 1.0 \times 10^{-8}$ Torr.

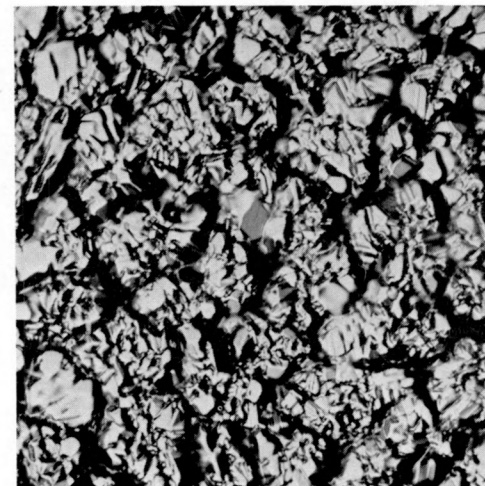
regions on the surface of 1-61-3, silicon grains as large as 200 microns were observed. Before removal from the SSC, four gold pads were evaporated on each of the three films so that electrical measurements could be made later.

2. Effects of Temperature. The next series of depositions on MoSi_2 substrates 1-71-1, 1-71-2 and 1-71-3 was designed to study the effects of temperature on silicon grain growth. As before, the substrates were mounted in tantalum heating envelopes and were annealed in-situ for 200 min at 1050°C . During the anneal, the maximum pressure attained was 3×10^{-8} Torr. Each deposition occurred at a base oxygen partial pressure which was below 5×10^{-13} Torr. For substrate 1-71-3, silicon was deposited at 650°C for 100 min at a rate of $\sim 500 \text{ \AA/min}$. The grain size of this deposit was below $1 \mu\text{m}$ in cross section and the surface, shown in Figure 14(a), gave a diffuse appearance. Silicon was deposited at a rate of 1000 \AA/min on substrate 1-71-1 for 100 min at a temperature of 950°C . The resulting deposit had grains of 2 to $80 \mu\text{m}$ in cross section with the larger grains located near the edges. Examining these large grains with the channeling technique showed that they were crystalline but randomly oriented. Figure 14(b) is a surface photograph of the center region of 1-71-1, and its surface was not significantly different than sample 1-61-3, shown in Figure 14(c) which was prepared at 1100°C .

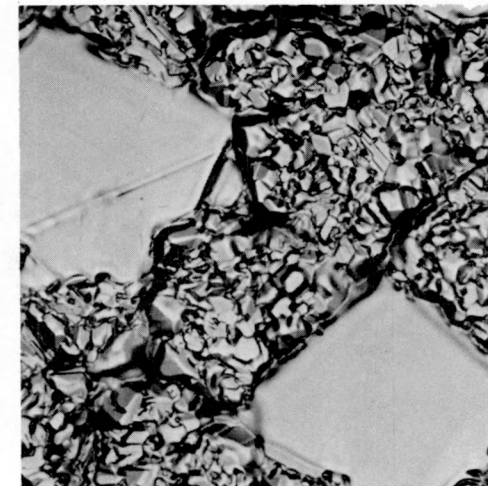
When silicon was deposited at 800°C for 100 min on substrate 1-71-2 at a rate of $\sim 1200 \text{ \AA/min}$, the resulting film possessed a "mottled" appearance that is readily seen in Figure 15. The diffuse and "smooth" regions that produced the "mottled" appearance were closely examined. Figure 16(a) and (b) illustrate three distinct surface morphologies. The surface shown in



a



b



c

Figure 14. Optical photomicrographs of silicon deposited on MoSi_2 substrates at base pressure showing the effects of temperature on grain growth. (a) Sample 1-71-3, with a deposition temperature, $T_D = 650^\circ\text{C}$, magnification 500X. (b) Sample 1-71-1 with $T_D = 950^\circ\text{C}$, magnification 500X. (c) Sample 1-61-3 with $T_D = 1100^\circ\text{C}$, magnification 500X.

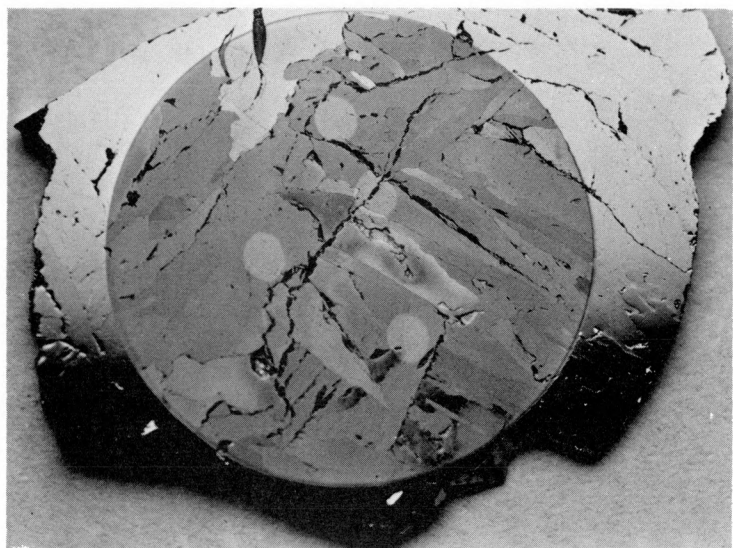


Figure 15. A photograph of sample 1-71-2 taken at 6X of silicon deposited at 800°C on MoSi₂. In the upper left corner an area of heteroepitaxial growth has a high reflectivity.

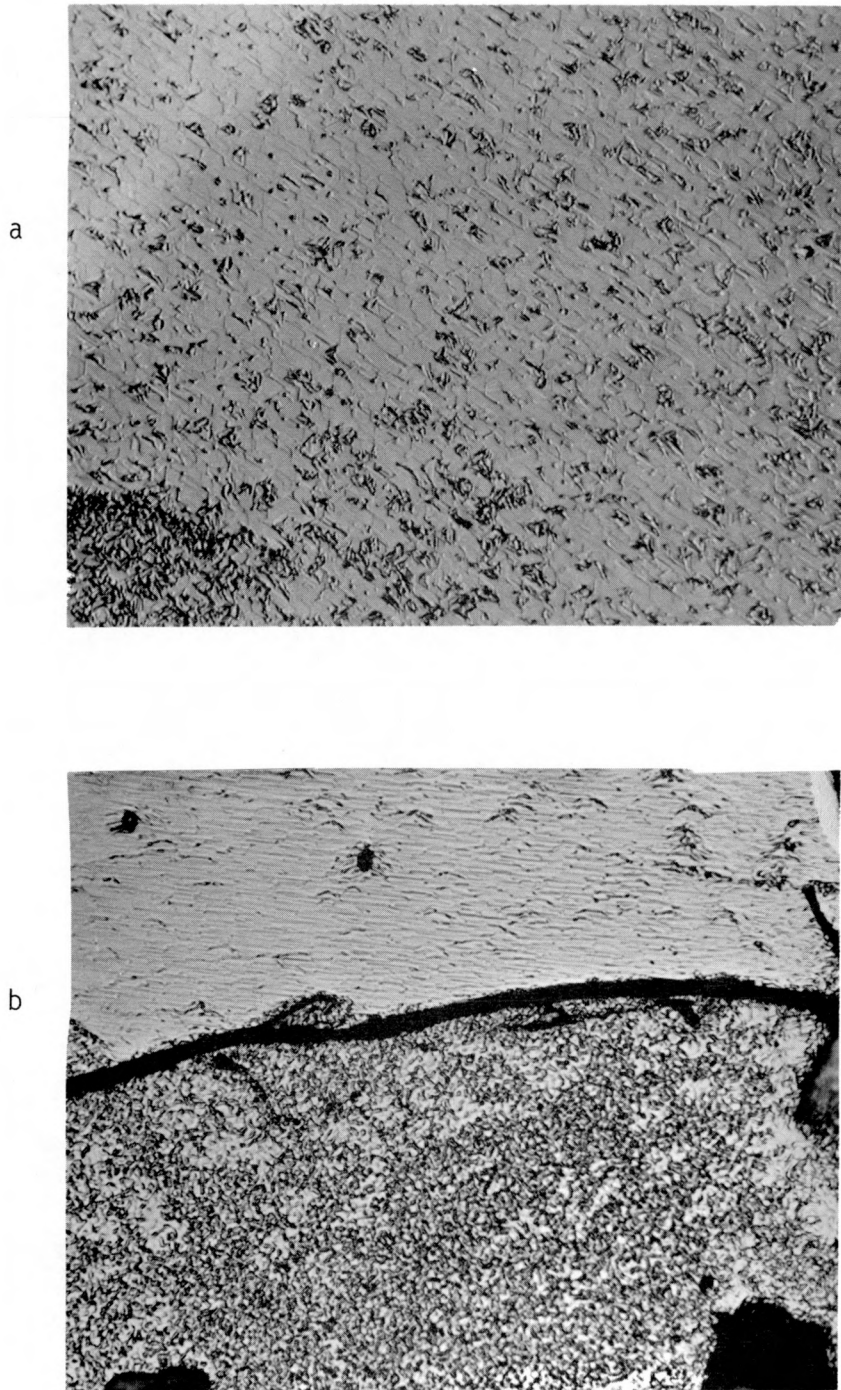


Figure 16. Optical photomicrographs of silicon deposited on MoSi₂ at 800°C on sample 1-71-2. (a) Photomicrograph of an area where hetero-epitaxial silicon was grown on {111} MoSi₂ planes, taken at 500X. (b) Photomicrograph showing different silicon morphology which was separated by grain boundary, taken at 500X.

Figure 16(a) was examined with x-ray and electron channeling techniques and the "terrace" like silicon features each produced identical channeling patterns. Thus, the silicon deposit in the entire field shown in Figure 16(a) is monocrystalline on a (111) MoSi_2 grain. In Figure 16(b), the two distinct morphologies are separated by a grain boundary. The smooth silicon was crystalline as confirmed by channeling techniques, and the diffused silicon was not. Based on these results we can state that heteroepitaxial silicon growth can be achieved at 800°C on (111) plane of MoSi_2 with a lateral extent of several millimeters.

In the next series of silicon depositions on MoSi_2 substrates the above effect was reexamined as a function of oxygen partial pressure. Three MoSi_2 substrates were first examined by x-ray diffractometry and electron channeling techniques to confirm the presence of {111} planes prior to loading in the SSC. Each substrate was annealed in-situ for 180 min at 1100°C and during each evaporation, the substrate temperature was maintained at 800°C.

For substrate 1-111-1, silicon was deposited at a rate of 215 Å/min for 300 min with the oxygen partial pressure measured as 6×10^{-13} Torr. The characteristic "mottled" pattern did not appear on this sample but silicon grains, shown in Figure 17(a) were measured at 2 to 20 μm in cross section. The experiment was repeated with substrate 1-111-2 in which the oxygen partial pressure was 1.6×10^{-13} Torr, but the deposition was for only 100 min at 180 °Å/min. In one region of this sample, heteroepitaxial silicon, shown in Figure 18, was grown in the (111) plane. These individual structures that composed this region were approximately 100 μm in cross section and were rotated slightly around the [111] direction. However, the substrate grain for this deposit was not of the (111) orientation as was the case for substrate 1-71-2.

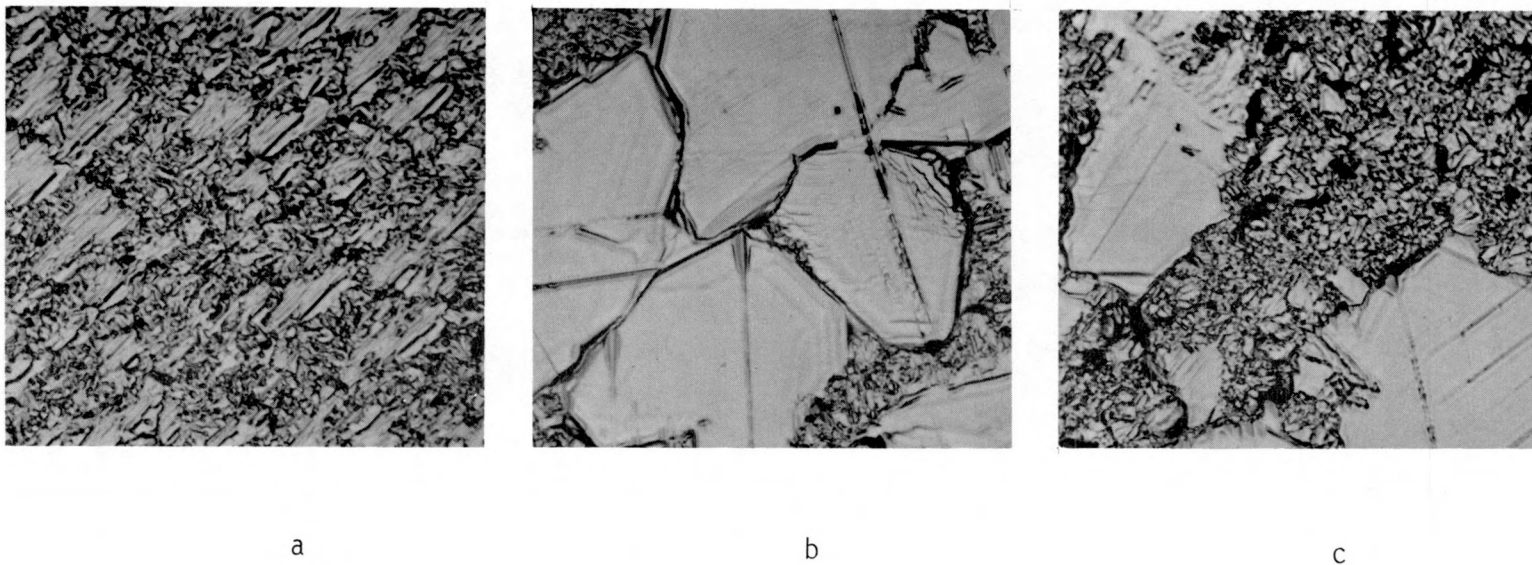


Figure 17. Optical photomicrographs of the silicon deposited on MoSi₂ in experiment 1-111 at 800°C. (a) Sample 1-111-1, silicon deposited in oxygen partial pressure, p_{O_2} , of 6.1×10^{-13} Torr, magnification 500X. (b) Sample 1-111-2, silicon deposited in $p_{O_2} = 1.6 \times 10^{-13}$ Torr, magnification 500X. (c) Sample 1-111-3, silicon deposited in $p_{O_2} = 1.6 \times 10^{-8}$ Torr, magnification 500X.

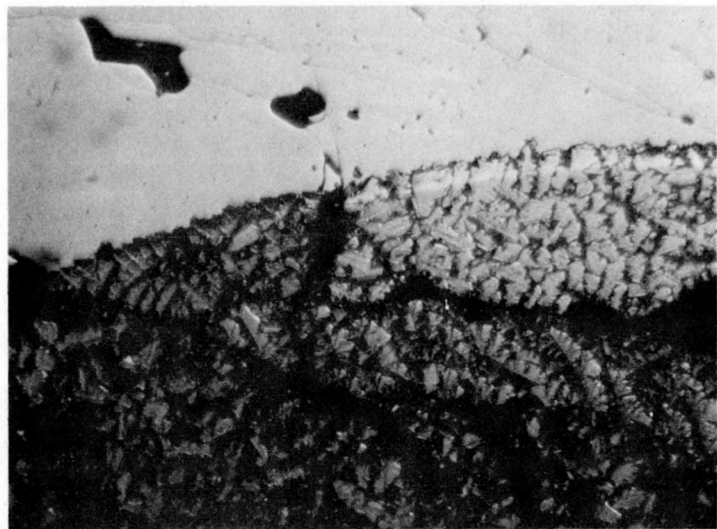


Figure 18. An optical photomicrograph of 1-111-2, taken at 50X, showing in the right corner heteroepitaxial {111} silicon on MoSi₂.

Shown in Figure 17(b) is another region of the surface of sample 1-111-2 which is covered with randomly oriented crystalline grains measuring 2 to 100 μm across. The deposition on the final MoSi_2 substrate 1-111-3 was for 100 min at 280 $\text{\AA}/\text{min}$ under an oxygen partial pressure of 1.6×10^{-8} Torr. The grains, shown in Figure 17(c), are crystalline and measured 2 to 80 μm in cross section but there was no evidence of heteroepitaxial growth on sample 1-111-3.

Silicon grown on molybdenum disilicide does not react with the substrate since there is no free metal available. The presence of oxygen has been shown to have a serious degrading effect on the growth of large grain silicon. At 800°C, heteroepitaxial silicon grew on (111) MoSi_2 . On a different substrate orientation, silicon grew with a (111) orientation. Above this temperature, silicon clustered to form large grains but this is not epitaxy since these were randomly oriented grains. At the lower temperature, 650°C, grains of less than one micron grew on the substrate. Oxygen present during the growth process prevented the heteroepitaxial growth of silicon and in some cases, reduced the formation of large silicon grains.

E. Electrical Characterization.

Our first electrical characterization was to determine the sign of the majority carriers in the film with a standard hot probe Seebeck coefficient tester. The three silicon deposits on MoSi_2 in Experiment 1-61 were found to be n-type. Current-voltage curves were obtained across the films between the metallic MoSi_2 substrates and the gold pads. The curves were linear or nearly linear indicating ohmic contacts for substrates 1-61-1 and 1-61-2. The reason for this is not clear.

Typical diode behavior was observed however for the 1-61-3 film when the gold contact was forward biased. A Schottky barrier was therefore present at the silicon-gold interface and the MoSi_2 -silicon interface was ohmic. Figure 18 shows a plot of current density vs voltage showing the typical exponential behavior. The saturation current density, J_s , determined at $V=0$, was used to calculate the barrier height, ϕ_B , from the equation:

$$\phi_B = \frac{kT}{q} \ln \left(\frac{AT^2}{J_s} \right)$$

where A is the effective Richardson constant. A value of $120 \text{ A/cm}^2/\text{K}^2$ was chosen for A ²⁹ from which a barrier height of 0.63 eV was calculated.

The insert in Figure 19 shows the I-V curve under both forward and reverse bias. Several effects can account for the shape of the curve in the reverse bias direction. When the barrier height is small, about half of the silicon band gap in this case, the Schottky emission current dominates at the reverse current and increases gradually with reverse bias. In addition, there may be edge leakage current around the gold pad which would also distort the reverse current curve.

The results of this I-V plot were reanalyzed according to the method of Norde³⁰ to determine the Schottky Barrier height in the presence of high series and high semiconductor resistance. Based on this analysis the recalculated barrier height was $\phi_B = 0.69 \text{ eV}$.

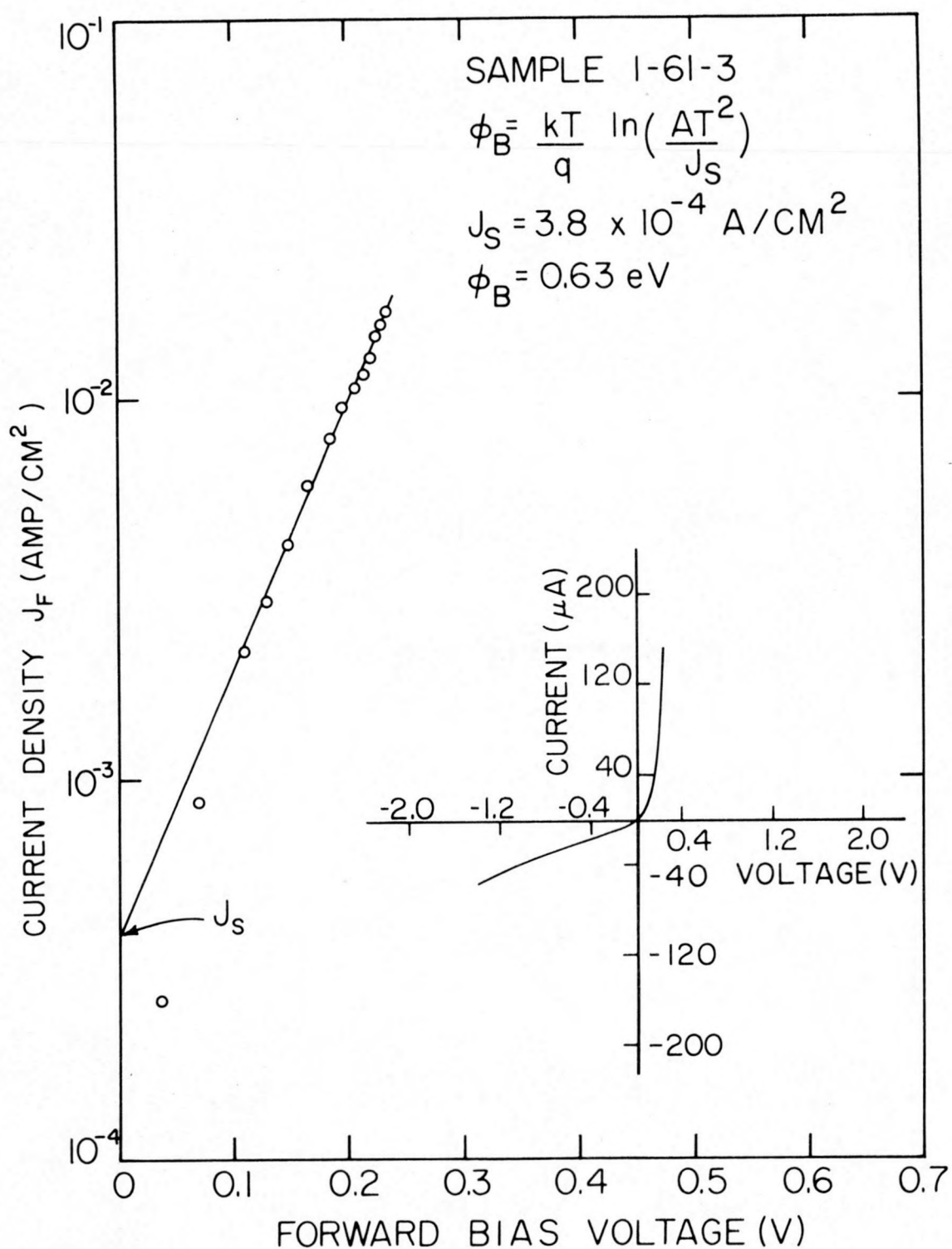


Figure 19. A plot of current density, J_F , versus forward bias voltage. Insert shows the current under forward and reverse bias. Barrier height was 0.63 eV.

SUMMARY AND CONCLUSIONS

This study produced three important results, namely: (1) the suppression of silicide growth by the use of a silicon source heavily doped with phosphorus, (2) the influence of oxygen partial pressure even at the 10^{-10} Torr level, on silicon grain size, and (3) the first known preparation of silicon heteroepitaxy on a metallic substrate, namely MoSi_2 . The discovery of these results followed from an understanding and control of those factors known to be important for enhancing silicon grain growth. These factors are: (1) deposition temperature, (2) substrate composition, (3) substrate orientation, and (4) ambient gas environment during operation.

In the absence of phosphorus in the silicon source and under an oxygen partial pressure in the 10^{-13} Torr range, silicon grains could only be grown on tungsten and molybdenum, among the least reactive metals with silicon, at temperatures below 650°C . At higher temperatures, the deposited silicon reacted completely to form silicide films leaving no free silicon. The silicon grains grown below 650°C were one micron or less in cross-section. The addition of phosphorus to the silicon source allowed silicon films to be deposited on tungsten, molybdenum and tantalum at temperatures as high as 750°C before silicide reactions prevented the formation of free silicon. On a single tantalum metal substrate, an additional one hundred degrees, from 650 to 750°C , produced nearly one order of magnitude increase in silicon grain size to a maximum of about five microns across. However, this grain size was too small for silicon solar cell fabrication and forced the consideration of bulk silicide substrates to completely suppress the silicide formation above 750°C by removing the free metal in the substrate or a potential reactant with the arriving silicon vapor.

The use of large grain polycrystalline MoSi_2 substrates was successful at suppressing silicide reactions as a factor in silicon grain growth even at temperatures as high as 1100°C . The silicon grain morphology, as deposited on MoSi_2 substrates, depended heavily on deposition temperature, partial pressure of oxygen present during deposition, and the orientation of the MoSi_2 grains. Above 950°C silicon films had grains measuring 80 microns across if the oxygen partial pressure was kept below 10^{-12} Torr. Little effect of the MoSi_2 grain orientation was evident under these conditions. At 1100°C , the addition of 10^{-10} Torr partial pressure of oxygen reduced the silicon grain size, by a factor of ten, to eight microns in cross-section. This effect of oxygen partial pressure, even at the very low level of 10^{-10} Torr, on the silicon grain size was one of the most important results of this entire study.

When the MoSi_2 substrate temperature was varied from 650°C to 950°C and the oxygen partial pressure was maintained at 4×10^{-13} Torr, significant changes in silicon grain morphology were observed. At 650°C , sub-micron silicon grains were found similar in appearance to those observed on pure molybdenum substrates. Little effect of the MoSi_2 grain orientation was evident. At 950°C , silicon grains many tens of microns across were found and again little evidence of MoSi_2 grain orientation effects was found. At 800°C however, the results were dramatically different. Large differences in silicon grain size were discovered as a function of MoSi_2 grain orientation. For (111) MoSi_2 grain, single crystal silicon films were grown several millimeters in cross-section, which is more than adequate for silicon solar cell fabrication. For other MoSi_2 grain orientations submicron

silicon grains were observed. The discovery of heteroepitaxial silicon growth on (111) MoSi_2 at 800°C represents the second most important result of this work. Subsequent depositions at 800°C on MoSi_2 substrates showed the effects of oxygen partial pressure, silicon deposition rate, and silicon thickness on the silicon film morphology. It has become clear that the preparation of heteroepitaxial silicon on MoSi_2 substrates requires very careful control of all of those parameters known to affect silicon grain growth.

RECOMMENDATIONS

Based on the results of this study we make the following recommendations:

1. Our discovery of the enhanced silicon grain growth on MoSi_2 at 1100°C for oxygen partial pressure below 10^{-10} Torr represents a significant research area for the utilization of a space vacuum facility for materials processing. It compares in significance to our reported ultrapurification of thorium by electrotransport processing at pressures below 10^{-10} Torr.³¹
2. The preparation of heteroepitaxial silicon on (111) grains of MoSi_2 at 800°C provides the basis for further extensive studies involving fabrication of large single crystals of MoSi_2 . These samples would permit detailed studies of the effects of silicon deposition rate, substrate temperature and oxygen partial pressure.
3. The role of phosphorus in suppressing the silicide formation rate is not understood. Further studies involving different source dopant concentrations should be pursued with special reference to the solid solubility of phosphorus in silicon and various silicide compounds so that a prediction of the phosphorus distribution in a growing silicon-silicide structure could be made.
4. Attempts to utilize other large grain polycrystalline silicides as substrates for silicon heteroepitaxy should be pursued vigorously. Candidate silicides should be selected from those already known to grow epitaxially from metal films on single crystal silicon such as Pd_2Si and FeSi_2 .

5. In addition to large grain polycrystalline forms of silicides such as FeSi_2 , elemental metals, e.g. iron, may be used to first grow thin films of the silicide on which the silicon film would be deposited.

BIBLIOGRAPHY

1. H. Kelly, *Science* 199 634 (1978).
2. W. A. Anderson, A. E. DeLahoy and R. A. Milano, *J. Appl. Phys.* 45 3913 (1974).
3. J. P. Ponpon and P. J. Seffert, *Appl. Phys.* 47 3248 (1970).
4. T. L. Chu, *Proceedings of NBS Workshop on Stability of Solar Cells*, NBS Special Publication 400-58, p. 41 (August 1979),
5. A. J. Bevolo, F. A. Schmidt, H. R. Shanks and G. J. Campisi, *J. Vac. Sci. Technol.* 16 13 (1979).
6. B. A. Joyce, *Rep. Prog. Phys.* 37 363 (1974).
7. W. K. Burton, N. Cabrera and F. C. Frank, *Phil. Trans. Roy. Soc.* 243A 299 (1950).
8. B. A. Unvala and G. R. Booker, *Phil. Mag.* 9 691 (1964).
9. G. R. Booker and B. A. Unvala, *Phil. Mag.* 11 11 (1965).
10. H. Widmer, *Appl. Phys. Letts.* 5 105 (1964).
11. F. Jona, *Appl. Phys. Letts.* 10 235 (1966).
12. F. Jona, Surfaces and Interfaces, Proc. 13th Sagomore Army Mat. Res. Conf., ed. J. J. Bush, N. C. Reed, and V. Weiss, p. 399, Syracuse Univ.
13. R. D. Henderson, W. J. Poliot and J. Simpson, *Appl. Phys. Letts.* 15 16 (1970).
14. R. C. Henderson, R. B. Marcus and W. J. Polito, *J. Appl. Phys.* 42 1208 (1971).
15. R. C. Henderson and R. F. Helm, *Surf. Sci.* 30 310 (1972).
16. J. M. Charig and D. J. Skinner, *Surf. Sci.* 15 277 (1969).
17. B. A. Joyce, R. R. Bradley, B. D. Watts and G. R. Booker, *Phil. Mag.* 19 403 (1969).
18. B. A. Joyce, J. H. Neave and B. E. Watts, *Surf. Sci.* 15 1 (1969).
19. B. A. Joyce, R. R. Bradley and G. R. Booker, *Phil. Mag.* 15 1167 (1967).

20. B. J. Bennett and R. W. Gale, Phil. Mag. 22 135 (1970).
21. J. J. Milek, Epitaxial Silicon and GaAs Thin Films on Insulating Ceramic Substrates, Electronic Properties Information Center, Hughes Aircraft Company, Culver City, CA (1968).
22. J. D. Filby and S. Nelson, (Single Crystal Films of Silicon in Insulators) British J. Appl. Phys. 18 1357 (1967).
23. C. C. Chang, J. Vac. Sci. and Tech. 8 500 (1971).
24. T. L. Chu, H. C. Mollenkopf and S. S. Chu, J. Electrochem. Soc. 123 106 (1976).
25. F. Jona, J. Appl. Phys. 42 2557 (1971).
26. F. Jona, J. Appl. Phys. 44 351 (1973).
27. F. Jona, J. Appl. Phys. 44 4240 (1973).
28. G. W. Racette and R. T. Frost, J. Cryst. Growth 47 384 (1979). Private communication.
29. S. M. Sze, Physics of Semiconductor Devices, Wiley Interscience, p. 395 (1969).
30. H. Norde, J. Applied Phys. 50 5052 (1979).
31. F. A. Schmidt, B. K. Lunde and D. E. Williams, Ames Laboratory Report No. IS-4125, January 1977.